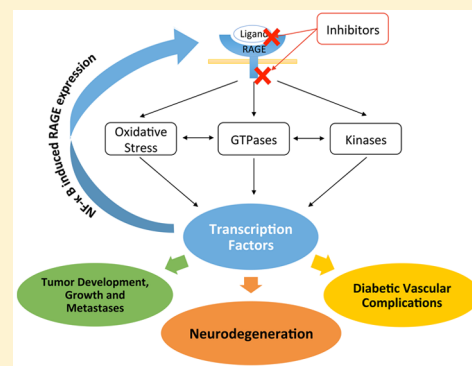


Targeting the Receptor for Advanced Glycation Endproducts (RAGE): A Medicinal Chemistry Perspective

Salvatore Bongarzone,* Vilius Savickas, Federico Luzi, and Antony D. Gee^{1b}

Division of Imaging Sciences and Biomedical Engineering, King's College London, King's Health Partners, St. Thomas' Hospital, London, SE1 7EH, United Kingdom

ABSTRACT: The receptor for advanced glycation endproducts (RAGE) is an ubiquitous, transmembrane, immunoglobulin-like receptor that exists in multiple isoforms and binds to a diverse range of endogenous extracellular ligands and intracellular effectors. Ligand binding at the extracellular domain of RAGE initiates a complex intracellular signaling cascade, resulting in the production of reactive oxygen species (ROS), immunoinflammatory effects, cellular proliferation, or apoptosis with concomitant upregulation of RAGE itself. To date, research has mainly focused on the correlation between RAGE activity and pathological conditions, such as cancer, diabetes, cardiovascular diseases, and neurodegeneration. Because RAGE plays a role in many pathological disorders, it has become an attractive target for the development of inhibitors at the extracellular and intracellular domains. This review describes the role of endogenous RAGE ligands/effectors in normo- and pathophysiological processes, summarizes the current status of exogenous small-molecule inhibitors of RAGE and concludes by identifying key strategies for future therapeutic intervention.



■ INTRODUCTION

Advanced glycation endproducts (AGEs) are produced by the nonenzymatic glycation of proteins upon exposure to reducing sugars.¹ Glycation leads to loss of enzymatic function, protein cross-linking, or aggregation.^{2,3} The accumulation of AGEs play an important role in many health disorders including diabetes mellitus, immunoinflammation, cardiovascular, and neurodegenerative diseases.^{4–9} AGEs mediate their pathological effects by activating signaling cascades via the receptor for advanced glycation end products (RAGE), a 45 kDa transmembrane receptor of the immunoglobulin superfamily prevalent at low concentrations in a variety of healthy human tissues, including the lungs, kidneys, liver, cardiovascular, nervous, and immune systems.^{10,11}

As a receptor for AGE and other proinflammatory ligands, RAGE has been investigated as a potential biomarker of numerous pathological conditions. Altered plasma or tissue level of various RAGE isoforms has been identified in patients with diabetic complications, cardiovascular diseases, and Alzheimer's disease.^{12–14} In vitro and in vivo studies have demonstrated the potential of RAGE as a therapeutic target in cancer, cardiovascular diseases, and neurodegeneration.^{7–9,15–17} Our review aims to summarize the knowledge pertaining to RAGE structure, isoforms, endogenous ligands, biological functions, and key inhibitor candidates, including those currently undergoing preclinical and clinical evaluation.^{17–19}

■ STRUCTURE OF RAGE

The full-length human RAGE consists of an extracellular (amino acid residues 23–342, Figure 1A), hydrophobic transmembrane (residues 343–363), and cytoplasmic domains (residues 364–404).²⁰ The extracellular structure of RAGE can be further subdivided into three immunoglobulin-like domains: a variable (V) domain (residues 23–116) and two constant C1 (residues 124–221) and C2 (residues 227–317) domains (Figure 1A).^{10,20–22} The structure of the V domain consists of eight strands (A', B, C, C', D, E, F, and G) connected by six loops forming two β -sheets linked by a disulfide bridge between Cys38 (strand B) and Cys99 (strand F).^{21,22} The C1 domain folds into a classical C-type Ig domain.^{21,22} The molecular surface of V and C1 domains is covered by a hydrophobic cavity and large positively charged areas. Several hydrogen bonds and hydrophobic interactions occur between the V and C1 domains forming an integrated structural unit.^{21–24} X-ray crystallography, NMR spectroscopy, and in vitro and in vivo studies have demonstrated that the joint VC1 ectodomain is implicated in the interaction with a diverse range of RAGE ligands of acidic (negatively charged) character, such as AGEs, S100/calgranulin family proteins, high mobility group box 1 (HMGB1), and β amyloid (A β).^{22–27} In addition, RAGE may undergo a ligand-driven multimodal dimerization or oligomerization mediated through self-association of V–V or C1–C1 domains.^{21,23,28–30} The stability of this diverse oligomerized VC1–ligand complex might provide an explanation for its

Received: January 12, 2017

Published: May 8, 2017

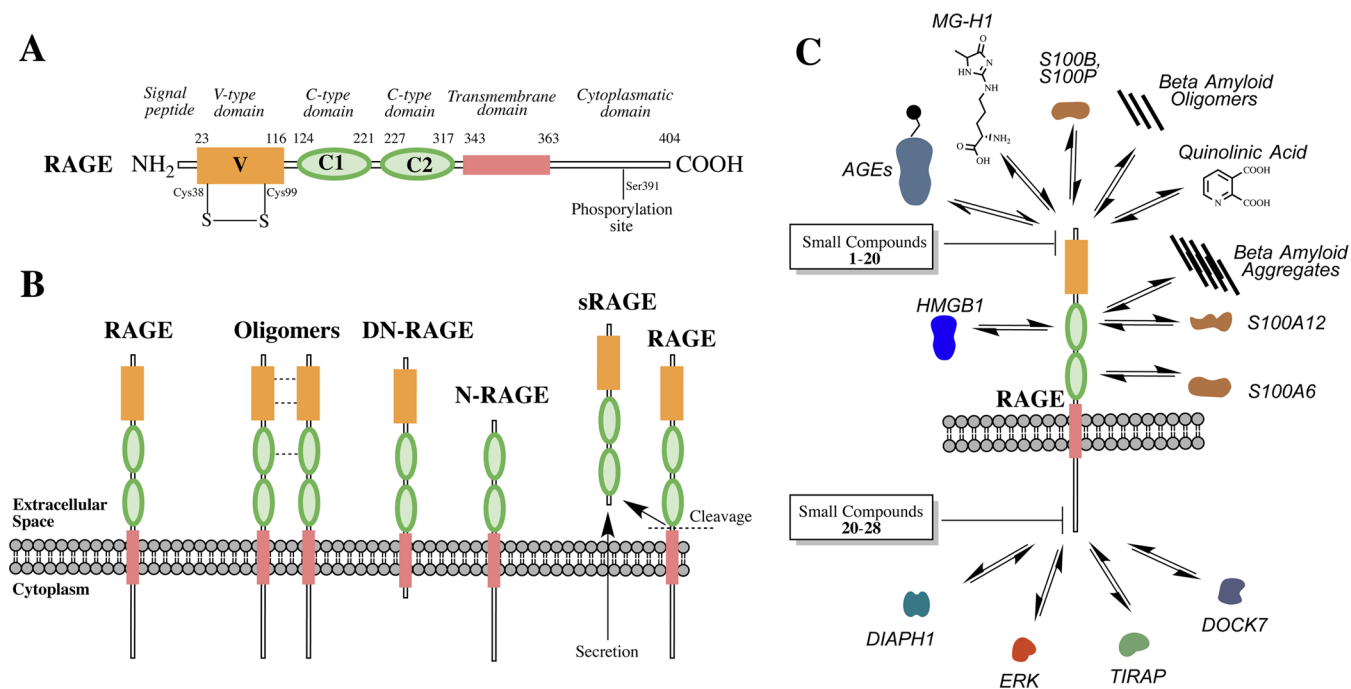


Figure 1. (A) Structure of full-length RAGE, including the variable (V) domain, constant (C1 and C2) domains, the transmembrane region, and the cytoplasmic tail. A disulfide bridge between Cys38 (strand B) and Cys99 (strand F) links the two β -sheets of the V domain. (B) RAGE isoforms. The key RAGE isoforms in the illustration include (from the left) the full-length RAGE, oligomerized full-length RAGE, dominant negative RAGE (DN-RAGE), N-truncated RAGE (N-RAGE), and soluble (secretory) RAGE (sRAGE). (C) The summary of extracellular ligands, intracellular effectors, and inhibitors binding to RAGE.

affinity/specificity for a wide-range of protein ligands and the resulting signal transduction.^{21,23,28–31}

In contrast to the VC1 complex, data from proteolysis, colorimetry, circular dichroism, and NMR experiments have described C2 as an independent structural unit flexibly connected to C1 via a 12-residue-long linker.²⁴ In analogy to the V domain, X-ray diffraction and NMR solution studies confirm that C2 exists as two- β sheets consisting of eight strands (A, A', B, C, E, F, G, and G') stabilized by disulfide bridges between strands B and F.²¹ However, the C2 structure also appears to include a large negatively charged surface with acidic residues directed toward the basic surface of the VC1 oligomer.²¹

The extracellular domain (VC1C2) of human RAGE (UniProtKB Q15109) shares a sequence identity of 79.6%, 79.2%, and 96.5% with mice (Q62151), rats (Q63495), and primates (*Rhesus macaque*; F1ABQ1), respectively.³² The positively charged residues involved in the binding of AGE to RAGE, including Lys52, Arg98, and Lys110, are conserved in all four species suggesting a common binding pattern.^{22,26,28}

Little is known about the transmembrane domain of RAGE, a helical structure containing a "GxxxG" motif, which may promote the helix–helix homodimerization of the receptor and thus may be involved in signal transduction.²¹ Sequence alignment and superimposition of the NMR-derived C-terminal of human RAGE with that of glycerol phosphate dehydrogenase GlpA structures, known to form a transmembrane helix dimer, shows a possible interaction between two GxxxG motifs involved in RAGE transmembrane helix homodimerization.²¹

The cytoplasmic tail of RAGE (364–404, Figure 1A) consists of 42 amino acids. This region is further divided into at least three parts: a membrane-proximal 17 amino acid domain rich in basic amino acids (Arg366, Arg368, Arg369, and

Glu371), a central 17 amino acid domain containing glutamic acids and a phosphorylation site at Ser391 and an unstructured C-terminus.^{33,34} NMR titration and in vitro binding studies have demonstrated that both structural regions are crucial for the interaction of the RAGE cytoplasmic domain with downstream effector molecules, including diaphanous-related formin 1 (DIAPH1), Toll-interleukin 1 receptor domain containing adaptor protein (TIRAP), and the extracellular signal-regulated kinase 1 and 2 (ERK 1/2). This results in downstream activation of the nuclear factor κ -light-chain-enhancer of activated B cells (NF- κ B) via the mitogen-activated protein kinase (MAPK) pathway.^{34–37} Because the RAGE cytoplasmic domain plays a significant mechanistic role in RAGE-induced signaling, truncation of this domain abolishes downstream RAGE activity, and decreases the associated pathological effects both in vitro and in vivo.^{38,39} The RAGE cytoplasmic domain of human RAGE shares a high sequence identity with primates (92%) and rodents (70.7%).³²

■ RAGE ISOFORMS

Because of extensive alternative splicing and metalloprotease-mediated cleavage, RAGE coexists as multiple transcript variants with differing ligand binding properties and diverse biological functions.^{40,41} In addition, a number of RAGE polymorphisms have been reported as potential disease biomarkers in human subjects.^{42,43} RAGE isoforms include the full-length RAGE, dominant negative RAGE (DN-RAGE, residues 23–363), N-truncated RAGE (N-RAGE, 124–404), and C-truncated secretory/soluble RAGE (sRAGE, 23–342).^{44,45}

The full-length RAGE (Figure 1B) contains all key receptor components and represents its active form to transduce the intracellular signal. RAGE binds numerous ligands and acts as a

Table 1. Intracellular Ligands Binding to RAGE

| ligand | RAGE isoform | RAGE binding domain | affinity for RAGE (K_d) | binding assay |
|--|---------------------|---------------------|--|---|
| CML/CEL modified peptides ^a | human sRAGE | V | 90–100 μ M | fluorescence titration ²² |
| | | | | NMR titration ²⁸ |
| MG-H ^b | human sRAGE | V | 30–40 nM | fluorescence titration ²⁶ |
| S100B ^c | human sRAGE | VC1 | 3.2–9.4 μ M | ITC |
| | | VC1 | $K_{d1} = 11$ nM, $K_{d2} = 244$ nM | SPR ²⁴ |
| | | V | $K_{d1} = 550$ nM, $K_{d2} = 470$ nM | |
| | | VC1 | $K_{d1} = 11$ nM, $K_{d2} = 200$ nM | SPR ⁷² |
| | | V | $K_{d1} = 0.5$ μ M, $K_{d2} = 0.6$ μ M | |
| | | V | $K_d = 8.3$ μ M (S100B dimer), $K_{d1} = 1.1$ μ M, $K_{d2} = 42$ nM (S100B tetramer) | SPR ⁶² |
| S100P | human RAGE | V | 6 μ M | ITC and fluorescence spectroscopy ⁷⁷ |
| S100A6 ^d | human sRAGE | VC1 | 0.6–5.8 μ M | SPR ⁷² |
| | | V | 0.5–13.5 μ M | |
| | | C2 | 28 nM to 1 μ M | |
| S100A12 | human sRAGE | C1 | 70 nM | fluorescence titration ²⁹ |
| HMGB1 (amphoterin) | rat and mouse sRAGE | VC1C2 | 6–10 nM | in vitro saturation binding assay ²⁷ |
| β amyloid ^e | human sRAGE | V | 70–80 nM | in vitro saturation binding assay ¹⁷ |
| quinolinic acid ^f | human and rat sRAGE | VC1 | 43 nM | fluorescence titration ⁸⁷ |

^aNMR structure of CEL-modified peptide with RAGE V domain reported in ref 22 (PDB 2L7U). ^bNMR complex of MG-H1 and RAGE V domain reported in ref 26. ^cNMR and docking calculation of S100B with RAGE VC1 domain reported in ref 23. ^dNMR (PDB 2M1K, ref 141) and X-ray (PDBs 4YBH and 4P2Y, ref 142) structures of S100A6 in complex with RAGE V and VC1C2 domains, respectively. ^eRAGE- β model complex predicted by protein–protein docking software reported in ref 83. ^fBinding mode of quinolinic acid and RAGE VC1 domain predicted by computational docking in ref 87.

key mediator in several downstream signaling cascades affecting immunoinflammatory responses, oxidative stress levels, cellular migration, proliferation, and apoptosis.^{17,25,37,40,46} These effects are likely to be potentiated by a positive feedback loop whereby initial RAGE activation leads to increased RAGE expression.^{47–52}

The absence of the cytoplasmic domain in DN-RAGE (Figure 1B) produces a “dominant negative” effect with a blunted signal transduction response to RAGE ligands.^{48,53} Overexpression of DN-RAGE attenuated HT1080 human fibrosarcoma cell proliferation and invasion in vitro and tumorigenesis in vivo.⁴⁸

The N-truncated isoform of RAGE (N-RAGE, Figure 1B) lacking the N-terminal V domain is incapable of interacting with AGEs because the V-domain is critical for their binding. However, the activation of N-RAGE might produce pathological effects through a pathway independent of the V-domain.⁵⁴

sRAGE (Figure 1B) is the circulating soluble form of RAGE which lacks the transmembrane and cytoplasmic domains. sRAGE consists of a heterogeneous population, comprising both isoforms generated from RAGE pre-mRNA alternative splicing (esRAGE) and the cleavage of RAGE extracellular domain from the cell surface receptor via matrix metal-

loproteinases.⁵⁵ sRAGE is the dominant form of the receptor counteracting RAGE-mediated pathogenesis by acting as a decoy.^{11,13,14,56} Translational human studies of pathological states, such as cardiovascular disorders or Alzheimer’s disease (AD), demonstrated their association with decreased blood plasma levels of sRAGE.^{13,14} The sequestering activity of sRAGE prevents ligand binding to RAGE, moderating the positive feedback-driven pathophysiological signaling pathway.^{57,58} The administration of sRAGE either peripherally or directly to target organs has been shown to reverse some of the RAGE-mediated pathological effects in vivo.^{47,56,58–60}

EXTRACELLULAR RAGE LIGANDS

Because of the presence of multiple domains (V, C1, and C2), receptor isoforms, and polymorphisms, RAGE is able to interact with a series of different ligands: from relatively low molecular weight AGEs, such as N_ϵ -carboxy-methyl-lysine (CML), N_ϵ -carboxy-ethyl-lysine (CEL), and methylglyoxal-derived hydroimidazolones (MG-H) to larger structures including $A\beta$ ($A\beta_{1-40}$ and $A\beta_{1-42}$) and proteins such as HMGB1, S100/calgranulins, $A\beta$ fibrils, and cross-linked/modified $A\beta$ (Figure 1C, Table 1).^{17,23,26,61–63} With its ability to bind such a diverse group of molecules, RAGE resembles a pattern recognition receptor, such as Toll-like receptors (TLR),

which are expressed on the cells of the innate immune system (e.g., macrophages) and are involved in the recognition of antigens presented by various pathogens.^{28,64} However, in contrast to TLR, RAGE ligands are of endogenous origin and typically accumulate in tissues during aging, inflammation, or in response to other tissue stresses.^{26,47,65–68}

CML and CEL. CML and CEL are two common endogenous AGEs found in humans which bind to the V domain of RAGE to trigger an immunoinflammatory response.^{1,22} In clinical studies of diabetes mellitus, high blood plasma levels of CML have been associated with enhanced RAGE expression.⁶⁹ Acidic peptide-bound CML and CEL appear to interact with positively charged (Lys52, Lys110, and Arg98) and hydrophobic residues of RAGE V domain (Table 1).^{22,28} However, NMR studies have shown that CML and CEL can only bind to RAGE if they are incorporated into larger peptide structures.^{22,28} The binding affinities (K_d) of such CML or CEL-containing peptides for the V domain of RAGE are reported to be around 100 μM with little dependence on the peptide chain modification (Table 1).^{22,28}

MG-H. An increased prevalence of methylglyoxal (MG) in vitro and in vivo has been linked to diabetic vascular complications with concomitant RAGE overexpression.⁷⁰

The NMR structural elucidation of an MG derivative (MG-H1) and RAGE reveals that MG-H1 forms charge–dipole and dipole–dipole interactions with the V domain (Figure 1C).²⁶ This binding begins a sustained period of cellular activation mediated by RAGE-dependent signaling such as increased phosphorylation of c-Jun N-terminal kinase (JNK) in vitro.²⁶ However, in contrast to CML or CEL, MG-H1 does not require an attachment to a peptide carrier to exert the effect and binds to RAGE with nanomolar affinity ($K_d = 40 \text{ nM}$, Table 1).²⁶ The imidazolone ring is found to be key to the interaction between MG-H analogues and residues on the V domain, particularly Lys52, Arg98, and Lys110, which are also involved in RAGE binding by CML/CEL.^{22,28}

S100/Calgranulin Family of Proteins. The S100/calgranulin family is a diverse group of Ca^{2+} -binding functional proteins involved in apoptosis, cell proliferation, differentiation, and immunoinflammatory response, showing varying affinities for different RAGE domains and triggering distinct cellular signaling pathways.^{71–73} S100B is a well-studied member of the family, which may act as a cytokine and has been implicated in both neurodegeneration and carcinogenesis.^{65,66} S100B exists as homo- or heterodimers with each subunit composed of two EF hand (helix–loop–helix) motifs.^{61,62} The binding of S100B to RAGE resembles that of AGEs because it docks around the positively charged surface of the VC1 domain, reflecting the acidic character of the ligand.^{23,72} The activation of RAGE signaling pathways by S100B is inhibited by sRAGE pretreatment.⁷⁴

Park and colleagues demonstrated that recognition of S100B by RAGE occurs via an entropically mediated process involving a Ca^{2+} -dependent hydrophobic interaction with the RAGE extracellular V and C1 domains.⁶¹ It has been demonstrated that S100B binding is highly influenced by the Ca^{2+} -dependent conformational change of the ligand, which undergoes oligomerization into hexamer or octamer complexes with Ca^{2+} in the human brain.^{61,62} Isothermal titration calorimetry (ITC) experiments showed that S100B recognizes RAGE by a Ca^{2+} ions dependent process.⁶¹ The measured binding affinity of S100B for sRAGE is influenced by its degree of oligomerization and the RAGE construct used in the assay.⁶¹

The K_d values of S100B for the V and VC1 domains of immobilized sRAGE are 0.5 μM and 11 nM, respectively (Table 1).^{24,72} A greater level of oligomerization (S100B tetramer versus S100B dimer) appears to generally improve the S100B binding affinity for RAGE and favors cell growth.⁶¹

The interaction between S100B– Ca^{2+} complex and RAGE homodimers also induces receptor oligomerization.⁷⁵ As recently demonstrated by Xue et al., this S100B-driven sRAGE oligomerization may in turn accommodate the interaction between RAGE and its intracellular effector proteins (e.g., DIAPH1), thereby initiating a downstream signaling pathway.⁷⁵

In analogy to S100B, S100P binds to the RAGE V domain and activates various signaling pathways (e.g., ERK, MEK, MAPK, and NF- κB) to promote tumor growth and metastasis.^{76–78} The Ca^{2+} -bound S100P homodimer interacts RAGE V domain with moderately strong affinity ($K_d = 6.0 \mu\text{M}$, Table 1), resulting in RAGE homodimerization.⁷⁷ The binding interface of RAGE and S100P overlaps with the region involved in S100B and AGEs interaction.^{23,77,79}

Calgranulin C (S100A12) is yet another cytokine-like member of the S100 family that, like S100B, binds Ca^{2+} forming dimers or hexamers, enabling a conformational change and leads to the ligation of RAGE through two hydrophobic surfaces.²⁹ However, in contrast to S100B, the fluorescence titrations and NMR spectra compiled by Xie et al. showed that the interaction between S100A12 and sRAGE occurs through the C1 domain without a significant involvement of either the V or C2 domains.²⁹

While binding to VC1 is favored by the majority of S100 ligands (e.g., S100B), surface plasmon resonance (SPR) and in vitro studies by Leclerc and colleagues show a preferential ligation of S100A6 for C2 compared with VC1.^{71,72} The binding of S100B and S100A6 to RAGE is also associated with two distinct effects on the downstream signaling pathway and opposite physiological effects in neuroblastoma cells.⁷² While both ligands increase the production of ROS, S100B binding to RAGE activates protein kinase B (AKT), the NF- κB pathway, and increases cell proliferation, whereas S100A6 binding induces the JNK/caspase 3 and 7 pathway, resulting in enhanced apoptosis.⁷²

HMGB1 (Amphoterin). HMGB1 is a “cytokine-type” RAGE ligand, produced by monocytes, that plays a role in inflammation, regulation of cell migration, and angiogenesis in vitro and potentially affects development of metastatic malignant disease in vivo.^{63,67,68} In addition to activating RAGE signaling, HMGB1 facilitates its inflammatory effects by binding to other pattern recognition receptors, such as TLR4 in macrophages, thus confirming the similarity between RAGE and TLRs.⁸⁰ Some of the HMGB1 activities may be mediated through its function as a binding enhancer between RAGE and other ligands (e.g., macrophage adhesion ligand-1).⁸¹ Similarly to S100B, HMGB1 is likely to form a helix–loop–helix structure and utilizes its acidity to ligate RAGE via the C-terminal.^{62,63} The RAGE-binding region on HMGB1 appears to lie between residues 150 and 183 with an in vitro K_d in the low nanomolar range (Table 1).^{27,63}

Beta Amyloid. An increasing number of studies describe the interaction between RAGE and various forms of $A\beta$, particularly $A\beta_{1-40}$ and $A\beta_{1-42}$ peptides, leading to neurodegeneration and cognitive decline.^{17,19,46,82} A molecular model of the dimeric $A\beta$ and V domain of RAGE proposes the formation of ionic interactions between the acidic negatively

Table 2. Extracellular Effectors Binding to Cytoplasmic RAGE Domain

| extracellular effectors | RAGE isoform | affinity for RAGE (K_d) (μ M) | binding assay | ref |
|------------------------------|----------------------|--|--|-----|
| DIAPH1 ^a | human RAGE | <10 | NMR | 34 |
| ERK 1/2 | human and mouse RAGE | | in vitro binding, gel shifting assay, C-terminal truncation | 36 |
| PKC ξ , TIRAP, and MYD88 | human RAGE | | in vitro binding, Western blotting, immunoprecipitation, kinase assay | 33 |
| DOCK7 | human RAGE | | liquid chromatography and electrospray tandem mass spectrometry, Western blotting, immunoprecipitation, in vitro cell migration and immunohistochemistry | 89 |

^aNMR structure of cytoplasmic RAGE domain in complex with DIAPH1 reported in ref 34.

charged surface of A β and the positively charged residues of the V domain.⁸³ The binding affinity of soluble A β to RAGE is concentration-dependent, with a K_d for ¹²⁵I-labeled A β _{1–40} of 75 nM.¹⁷ A mouse transgenic model of AD showed that A β binds to RAGE, resulting in transport of A β from the bloodstream across the blood–brain barrier (BBB) and into the central nervous system (CNS) while RAGE inhibition suppresses the accumulation of A β in the brain.⁸⁴ The interaction of A β with RAGE in neuronal and endothelial cells induces oxidative stress and activates NF- κ B.⁸⁵

Moreover different A β conformational states, A β oligomers, fibrils, and aggregates interact in distinct RAGE binding sites.²⁵ In cell assays, oligomers and aggregates induce apoptosis through RAGE by activating caspase signaling and DNA fragmentation. RAGE-mediated A β oligomer- and aggregate-induced apoptosis requires the specific antagonism of the V and C1 domain of RAGE, respectively.²⁵

Quinolinic Acid. Quinolinic acid, a neuroactive metabolite of the kynurenine pathway, produces its neurotoxicity by overactivating the NMDA receptor, causing energy deficits, oxidative stress, and cell death.⁸⁶ The excess of quinolinic acid has been implicated in the development of various neurodegenerative disorders such as AD and Huntington's disease.⁸⁶ More recently, quinolinic acid has been investigated as a putative endogenous RAGE ligand.^{87,88} Flexible docking studies with quinolinic acid on human and rat VC1 domains by Serratos and co-workers identified the binding pattern across seven sites, including the CML/CEL and MG-H binding loci.^{22,26,87} Using fluorometric measurements, the K_d of quinolinic acid for VC1 was estimated to be approximately 43 nM (Table 1).⁸⁷ The effects of in vivo administration of quinolinic acid to rats activated the RAGE pathway, producing increased levels of oxidative stress, lactate dehydrogenase, and nitric oxide, enhanced expression of RAGE, COX-2, and NF- κ B, and led to dose-dependent neuronal death in the striatum.^{87,88}

INTRACELLULAR RAGE EFFECTORS

Despite the focus on the VC1 ectodomain of RAGE as the primary ligation site, the cytoplasmic domain of RAGE is essential for RAGE-mediated signaling and overall RAGE function. Recent reports employed a more holistic approach of evaluating the protein effector interactions encountered by the cytoplasmic domain of RAGE, including DIAPH1, ERK 1/2, TIRAP, and dedicator of cytokinesis 7 (DOCK7).^{33–35,37,89}

While in vitro-focused research to date has demonstrated the necessity of RAGE cytoplasmic tail binding to its intracellular adaptor proteins in order to facilitate the downstream signaling cascade, little is known about the specific binding sites of such molecules or the affinity at which this binding occurs. Future studies may therefore benefit the field by exploring the docking

patterns and affinity of molecules for ERK, TIRAP, and DOCK7 in order to explore them as potential targets for therapeutic intervention.

DIAPH1. DIAPH1 is one of the proteins that binds to the cytoplasmic tail of RAGE and has proven essential for RAGE-induced downstream signaling.^{35,37} Because DIAPH1 is also involved in actin and microtubule polymerization, it may play a direct role in tumor growth and its metastatic potential.⁹⁰ As could be anticipated, inhibition of RAGE–DIAPH1 complex formation successfully reduces the ligand-binding (e.g., CML) induced effects in vitro and in vivo.^{34,35} This demonstrates the importance of such protein–protein interactions in downstream signaling cascades (e.g., ERK and AKT pathways), cell migration and division, production of inflammatory cytokines (e.g., TNF- α), and direct myocardial ischemia.^{34,35} Solution NMR spectroscopy and site-directed mutagenesis identified that the DIAPH1 FH1 domain interacts with the small positively charged patch formed by Gln364, Arg365, Arg366, and Gln367 on the RAGE cytoplasmic tail ($K_d < 10 \mu$ M, Table 2).³⁴

ERK. In vitro binding experiments by Ishihara and co-workers confirmed that the cytoplasmic tail bound both phosphorylated and nonphosphorylated versions of ERK 1/2, suggesting a direct interaction between the receptor's intracellular domain and the kinases.³⁶ RAGE stabilizes ERK under the membrane-proximal cytoplasmic region and leads to activation of the interaction between ERK and other proteins.³⁶ Consistent with these results, the HMGB1-induced kinase activity of ERK is significantly more pronounced in RAGE-expressing cells.³⁶ Similarly to DIAPH1, this demonstrates the importance of simultaneous extracellular and intracellular RAGE ligation for the activation of its subsequent downstream pathways.^{34,36}

PKC ξ , TIRAP, and MyD88. A study by Sakaguchi et al. endeavored to answer the question of whether DIAPH1 and ERK are the only RAGE effectors involved in facilitating RAGE intracellular signaling pathways.³³ In vitro experiments in various cell lines confirmed that the extracellular activation of RAGE triggered the binding of protein kinase C ξ (PKC ξ) to the cytoplasmic domain, thereby resulting in RAGE phosphorylation at Ser391.³³ This process exhibited a dose-dependency of the extracellular ligands, such as S100A11, S100A12, HMGB1, and AGE, and was exclusive to RAGE, demonstrating its potential involvement in inflammation, immune responses, and other cellular functions.³³

Phosphorylation at Ser391 influences the RAGE binding of other intracellular effectors, particularly TIRAP and myeloid differentiation primary response gene 88 (MYD88).³³ As anticipated and in analogy to DIAPH1, this protein–protein interaction produced an increase in the activity of downstream RAGE signaling mediators such as NF- κ B, JNK, Rac1, AKT,

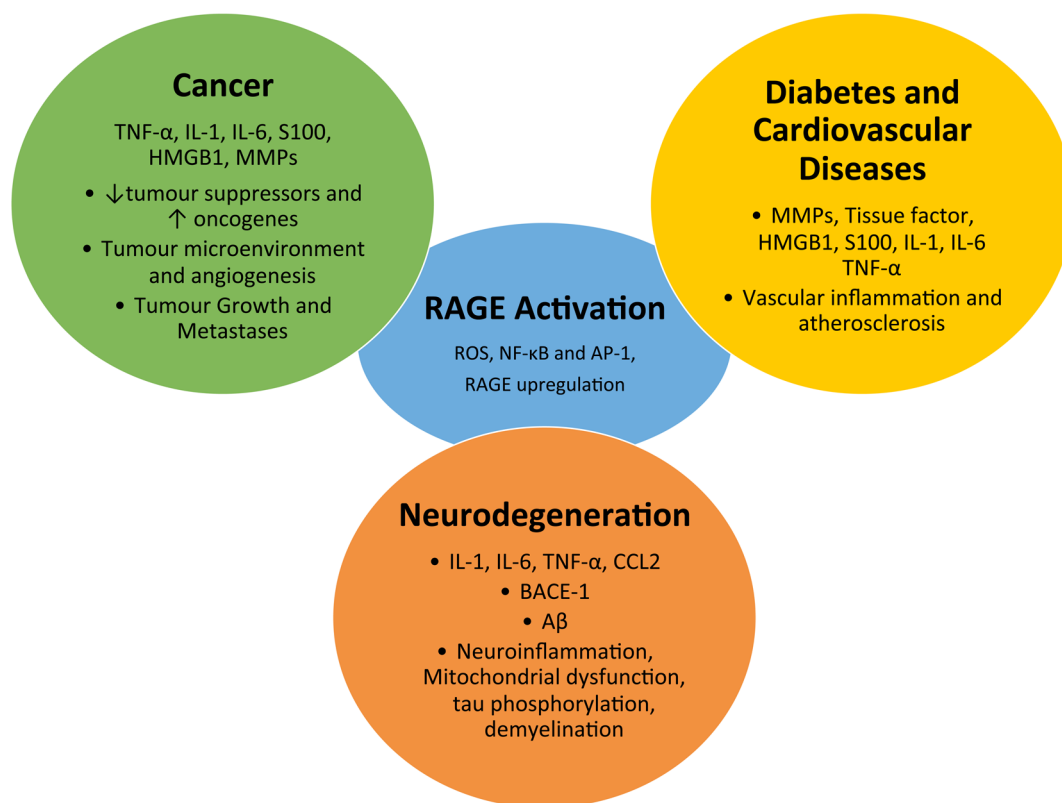


Figure 2. Schematic representation of signaling pathways activated by RAGE in cancer, cardiovascular diseases, and neurodegeneration.

and p38.³³ The inhibition of TIRAP, MYD88, or PKC ξ activity in endothelial cells resulted in a decreased production of secondary RAGE effector molecules, such as the epidermal growth factors IL-1 and IL-6, which are involved in inflammation and carcinogenesis.^{15,91} While the binding of TIRAP and MYD88 by RAGE proved its similarity to the aforementioned TLRs, Sakaguchi et al. showed the preference of RAGE for these adaptor proteins over other TLR ligands.³³

DOCK7. Employing immunoprecipitation and affinity purification followed by mass spectrometry, it was discovered that DOCK7 is an intracellular effector of RAGE.⁸⁹ As expected, endogenous DOCK7 binds to RAGE but not to DN-RAGE in HEK293T cells.⁸⁹ DOCK7 is involved in the activation of the GTPases such as Cdc42.^{89,92} The downregulation of DOCK7 resulted in marked interference with signal transduction from RAGE to Cdc42, indicating the involvement of DOCK7 in the RAGE-Cdc42 signaling axis in human cancer cell lines.⁸⁹

■ THE INVOLVEMENT OF RAGE IN DISEASE PROCESSES

RAGE is expressed in vascular smooth muscle, mesangial, endothelial, and lung alveolar epithelial cells, mononuclear phagocytes, and neurons.^{11,93} Overexpression and activation of full-length RAGE has been linked to neurodegenerative disorders,^{5,8,9,50} diabetic nephropathy, and nondiabetic vascular disease,^{12,94,95} acute liver and lung injuries,^{96–98} and malignant tumors.¹⁵ The interaction of RAGE ligands with the extracellular domain of RAGE initiates a downstream intracellular cascade mediated through multiple mechanisms, including the production of ROS and activation of ERK 1/2, Janus kinase (JAK), transducer and activator of transcription (STAT), Rho family of GTPases, MAPK, phosphatidylinositol

3-kinase (PI3K), AKT, and transcription factors (AP-1 and NF- κ B).^{9,17,37,48,49,51,99,100} Once activated, transcription factors migrate into the nucleus, interact with the DNA and lead to increased expression of pro-inflammatory cytokines, enzymes, as well as oncogenes with associated downregulation of tumor suppressor genes.^{101–103} In turn, this cascade generates overexpression of RAGE and its ligands, such as AGEs, S100B, and HMGB1, which leads to a positive feedback loop and further RAGE upregulation.^{47–52}

Tumorigenesis and Malignancy. In tumors, endothelial, lymphocytic, myeloid, and myeloid-derived suppressor cells, RAGE activation exerts gene upregulation and production of S100 family proteins and inflammatory cytokines (e.g., TNF- α , IL-1, and IL-6) via the NF- κ B/AP-1 signaling cascade, promoting angiogenesis (VEGF), tumor growth, and metastasis (Figure 2).^{15,73,104} The stimulation of RAGE in colorectal cancer cells by S100P proteins leads to NF- κ B/AP-1 activation through mitogen-activated protein kinase kinase (MEK), ERK phosphorylation, and increased expression of oncogenes such as microRNA-155.^{73,105} Antagonism of RAGE activity with either the anti-RAGE antibody or the antagonist derived from HMGB1 results in a pronounced reduction in cell growth, migration, and invasiveness.^{73,105} The administration of HMGB1 to human fibrosarcoma cells overexpressing RAGE activates Rho GTPases (Rac1 and Cdc42) and subsequently transcription factors (NF- κ B), exacerbating the malignant cellular phenotype in vitro and in vivo.⁴⁸

RAGE and the proinflammatory ligand S100A7 are co-overexpressed in aggressive clinical breast cancer cases.¹⁶ RAGE mediates S100A7-induced breast cancer growth and metastasis by activation of ERK and transcription factors that induce the expression of metalloproteinases (MMPs), enzymes involved in angiogenesis and metastatic disease progression.¹⁶ In turn, the

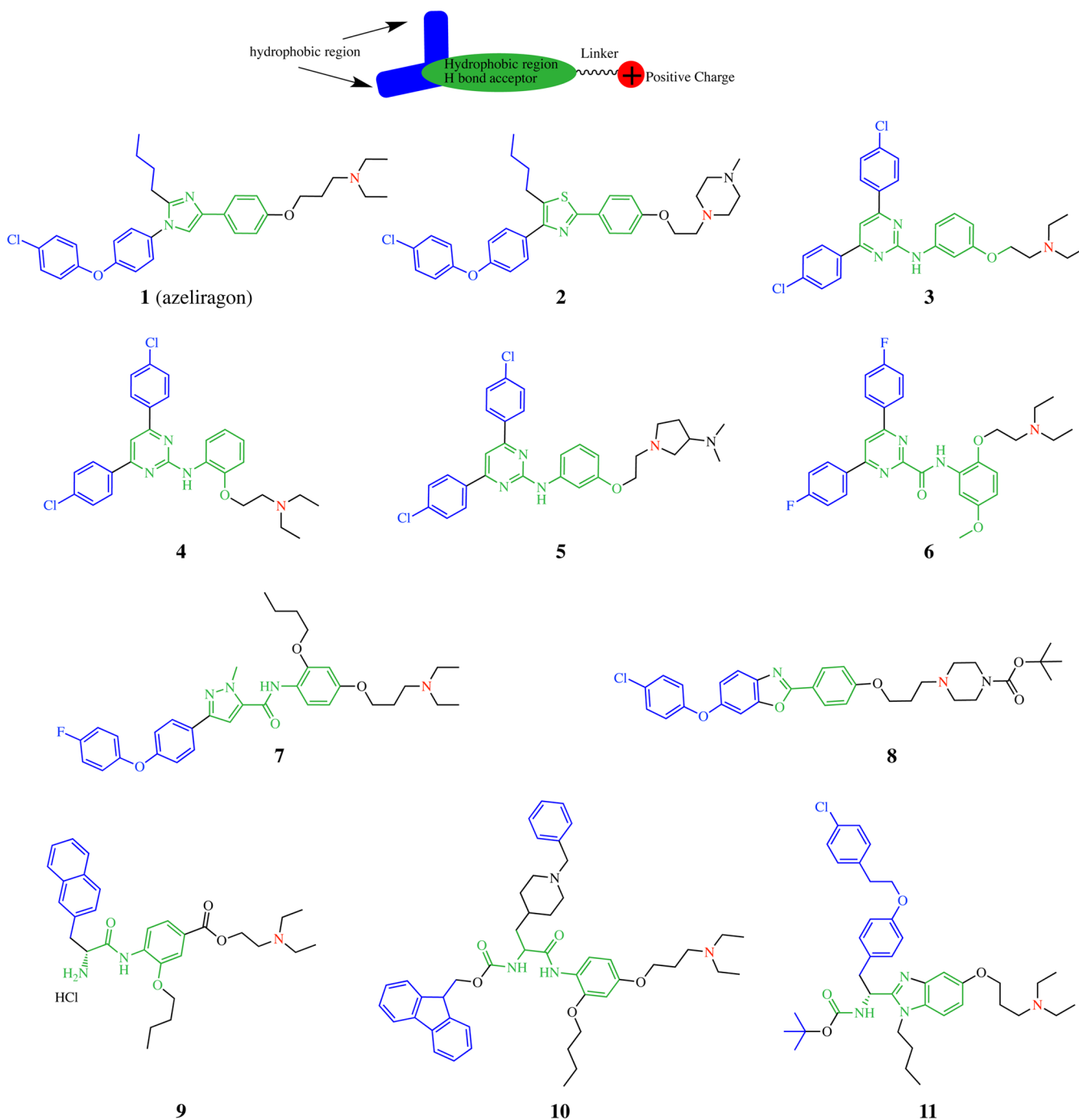


Figure 3. Chemical structures of RAGE inhibitors. Inhibitors 1–11 have a common pharmacophore which comprises: (1) a central heteroaromatic core capable of hydrogen bonding (green), (2) one or two hydrophobic regions (blue), and (3) a protonable nitrogen atom (red) connected to the central core by an alkyl linker.

administration of an anti-RAGE antibody or sRAGE to S100A7-expressing transgenic mice inhibited further tumor development and metastasis, whereas RAGE knockout mice demonstrated lower activation of the ERK/NF- κ B pathway.¹⁶

Diabetes and Cardiovascular Disease. RAGE and expression of its proinflammatory ligands have been implicated in chronic inflammation conditions such as atherosclerosis, diabetic complications, and nondiabetic vascular disease (Figure 2).^{12,94,106} Increased expression of RAGE, vascular cell adhesion protein 1, tissue factor, and MMPs has been demonstrated in aorta and kidney of diabetic mice.^{94,106} The

activation of chronic inflammatory signaling pathways compromises vascular integrity and stimulates the clotting cascade causing cardio- or renovascular damage.^{8,107} In diabetic rats such effects are exacerbated by AGE-induced cytosolic ROS production that facilitates mitochondrial superoxide production.¹⁰⁸

RAGE and its ligands are implicated in the pathogenesis of ischemia–reperfusion injury in the heart. In a murine model subjected to myocardial ischemia, RAGE activity coincided with enhanced expression of JNK or STAT5, the activators of the NF- κ B pathway.¹⁰⁹ Pharmacological blockade of RAGE

Table 3. Small Molecule Inhibitors of RAGE

| compd | RAGE domain | RAGE inhibition | effects | in vitro cellular assays | in vivo studies | ref |
|-------|-------------|--|---|--|--|--------------------|
| 1 | V | $K_d = 500$ nM (fluorescent polarization with sRAGE) | <ul style="list-style-type: none"> • $A\beta$ S100B, HMGB1, and CML-RAGE binding inhibition (in vitro) • reduction in inflammatory markers (in vitro) • decrease amyloid deposition and cognitive loss (in vivo) | | <ul style="list-style-type: none"> • APP^{Swe}Lon mice • mouse model of systemic amyloidosis | 19,121,122,143,144 |
| 2 | | $IC_{50} = 1.21$ μ M (ELISA on human RAGE- $A\beta$) | <ul style="list-style-type: none"> • RAGE-$A\beta$ binding inhibition • inhibition of $A\beta_{1-42}$ influx in the brain • inhibition of $A\beta_{1-42}$-associated NF-κB activation (in vitro) | <ul style="list-style-type: none"> • brain endothelial cells for BBB influx • CHO cells for neuroinflammation inhibition | | 123 |
| 3 | V^{42} | $K_d = 102$ μ M (SPR using human RAGE) $IC_{50} = 16.5$ μ M (ELISA on human RAGE- $A\beta_{1-42}$) | <ul style="list-style-type: none"> • downregulation of $A\beta$-induced NF-κB (in vitro) • cell survival (10 μM) = 37.3% (in vitro) • inhibition of $A\beta$ accumulation in the brain (in vivo) • improvement of cognitive function (in vivo) | <ul style="list-style-type: none"> • C6 glioma cells for $A\beta$-induced neuroinflammation inhibition • cytotoxicity in hippocampal HT22 | <ul style="list-style-type: none"> • wild-type mice for $A\beta$ brain entry • APP^{swe}/PS1 mice | 124,125 |
| 4 | V^{42} | $IC_{50} = 4.6$ μ M (ELISA on human RAGE- $A\beta_{1-42}$) | <ul style="list-style-type: none"> • downregulation of $A\beta$-induced NF-κB (in vitro) • inhibition of $A\beta$ accumulation in the brain (in vivo) | C6 glioma cells for $A\beta$ -induced neuroinflammation inhibition | wild-type mice for $A\beta$ influx | 124 |
| 5 | V^{42} | inhibitory activity > 4, at 20 μ M (ELISA on human RAGE- $A\beta_{1-42}$) | | | | 126 |
| 6 | V^{42} | inhibitory activity > 4, at 20 μ M (ELISA on human RAGE- $A\beta_{1-42}$) | cell survival (10 μ M) = 100.4% in HT22 cells | cytotoxicity in hippocampal HT22 | | 125 |
| 7 | V^{42} | $K_d = 43.4$ μ M (SPR) $IC_{50} = 1.9$ μ M (ELISA on human RAGE- $A\beta_{1-42}$) | cell survival (10 μ M) = 10.3% HT22 cells | cytotoxicity in hippocampal HT22 | | 125,127 |
| 8 | | 40% inhibition at 4 μ M against human RAGE- $A\beta_{1-42}$ interaction (FRET assay) | <ul style="list-style-type: none"> • RAGE-$A\beta_{1-42}$ binding inhibition (in vitro) • block $A\beta$ transport across the BBB (in vivo) • reduce amyloid deposition (in vivo) | hippocampal HT22 for cell survival | APP ^{swe} /PS1 mice | 128 |
| 9–11 | | $IC_{50} < 4$ μ M (ELISA on sRAGE and S100, $A\beta$, CML) | | | | 129,130,132 |
| 12 | V^{42} | K_i for 125 I- $A\beta_{1-40} = 25$ nM (RAGE-CHO cells) | <ul style="list-style-type: none"> • inhibition of $A\beta$ influx in the brain (in vivo) • low cytotoxicity in vitro and in vivo | <ul style="list-style-type: none"> • RAGE-CHO cells for cytotoxicity, oxidative stress and NF-κB activation • SH-SSYS cells for BACE1 expression | <ul style="list-style-type: none"> • APP^{swe}/0 mice • Wistar rats treated with AGEs | 17,46 |

Table 3. continued

| compd | RAGE domain | RAGE inhibition | effects | in vitro cellular assays | in vivo studies | ref |
|-------|---------------------------------|---|--|--|---|---------|
| 13 | V ⁴ | K _d = 15 nM (quantitative autoradiography) | <ul style="list-style-type: none"> blocked RAGE actions at the BBB and in the brain reduced Aβ₁₋₄₀ and Aβ₁₋₄₂ levels in brain normalized cognitive performance and cerebral blood flow in aged APP^{sw/0} mice reduced Aβ₁₋₄₀-induced NF-κB activation, BACE1 expression, cytokines (in vitro and in vivo) inhibited Aβ₁₋₄₀, Aβ₁₋₄₂, S100B, HMGB1 binding to RAGE (in vitro) | | | 18 |
| 14 | V ⁴ | K _d = 24 mM (microscale thermophoresis on human RAGE and Aβ ₁₋₄₂) | <ul style="list-style-type: none"> reduced Aβ₁₋₄₂, NF-κB, BACE1 and cytokines (in vitro and in vivo) normalizes cognitive functions (in vivo) | RAGE-overexpressing SH-SY5Y cells for cytotoxicity and neuroinflammation inhibition | APP ^{sw} /PS1 mice | 135 |
| 15–17 | VC1C2 | K _d = 0.2 nM (15), 0.6 nM (16), 3.1 nM (17) (SPR on human RAGE) | <ul style="list-style-type: none"> inhibition of lung colonization by tumor cells | LLC and B16 melanoma cells for metastasis inhibition | C57BL/6 mice for metastasis | 136,137 |
| 18 | VC1C2 | K _d = 1.69 nM (ELISA on human RAGE) IC ₅₀ = 412.7 nM (ELISA on human RAGE-CML-BSA) IC ₅₀ = 274.5 nM (ELISA on human RAGE-S100B) IC ₅₀ = 79.6 nM (ELISA on human RAGE-HMGB-1) | <ul style="list-style-type: none"> inhibition of U937 monocytes binding to RAGE (in vitro, IC₅₀ = 7.6 nM) reduction of LL-37-induced erythema (in vivo) | U937 monocytes | Balb/c mice for cutaneous inflammation | 137 |
| 19 | VC1C2 | | <ul style="list-style-type: none"> inhibition of NF-κB, inflammation, tumor growth and metastasis | pancreatic cancer cell lines | immune-deficient mice implanted with cancer cells | 138 |
| 20–28 | cytoplasmic domain ^c | K _d between 0.3 and 32 nM (native tryptophan fluorescence on human cytoplasmic domain of RAGE) | <ul style="list-style-type: none"> decreased cytokines and cell migration (in vitro and in vivo) increased left ventricular developed pressure (LVDP) after ischemia damage (ex vivo) | <ul style="list-style-type: none"> primary murine aortic smooth muscle cells primary murine aortic endothelial cells human macrophage-like THP1 cells | C57BL/6j mice activated with CML | 35,139 |

^aBinding modes of 3–7 and 14 with the RAGE V domain have been predicted by molecular docking calculations. ^bInteraction of 12 with the RAGE V domain has been identified using V domain-specific antibodies. ^cInteraction between 20–28 and the cytoplasmic RAGE domain has been identified by NMR.

activation with ursodeoxycholic acid exerts an antiatherogenic activity in diabetic mice, whereas administration of sRAGE protects them against ischemia–reperfusion injury.^{109–111}

Neurodegeneration. Because numerous neurodegenerative disorders, such as Alzheimer's, Parkinson's, Huntington's diseases, and amyotrophic lateral sclerosis, have been linked with neuroinflammation, multiple research studies have attempted to elucidate the role of RAGE physiology in their development.^{9,112} Immunohistochemical studies with human brain tissue have demonstrated that RAGE levels are increased in AD patients versus controls.^{113,114} In AD patients, RAGE expression is present on cerebral endothelial cells, astrocytes, and neurons of the hippocampus, entorhinal cortex, and superior frontal gyrus but absent in the cerebellum.^{113–116}

In neurodegenerative disorders RAGE is implicated in the amyloidogenic pathway as well as independent neurotoxic immunoinflammatory cascades (Figure 2).^{8,9,45,82} The binding of endogenous ligands, such as AGE, S100, or A β , to physiologically expressed RAGE, leads to its overexpression in neurons, microglia, astrocytes, and the vasculature of the BBB.^{9,17,45,112,117}

The increased presence of RAGE at the BBB leads to influx of A β and monocytes into the brain, whereas in neurons it enhances the activity of the A β -producing β -secretase enzyme (BACE1), induces tau hyperphosphorylation, neuroinflammation, and impairs neuronal function.^{17,84,117,118}

Accumulation of A β _{1–40} and A β _{1–42} in the brain results in the formation of oligomers and plaques inducing RAGE-mediated apoptosis in neurons.^{9,17,25,45,82,119} In vitro microglial models confirmed that RAGE-S100B interaction leads to the activation of the Rac-1/JNK axis and transcription factors (NF- κ B and AP-1).¹⁰³ This increases in vivo hippocampal and cortical brain production of BACE1 and the microglial/neuronal release of inflammatory markers, such as TNF- α , IL-1, IL-6, and chemokine (C–C motif) ligand 2 (CCL2).^{17,46,102}

Because RAGE remains activated as long as A β peptide and A β oligomers are present, RAGE may be involved in initiation and amplification of A β neuronal toxicity.⁸² Takuma et al. demonstrated that RAGE also contributes to the translocation of A β _{1–40} from the extracellular to the intracellular space, spreading among the cells and causing neuronal damage.¹²⁰ As expected, the inhibition of RAGE activity shows a pronounced drop in both in vitro and in vivo levels of brain ROS as well as improved cognitive function in animals and AD patients.^{17,46,121}

■ DEVELOPMENT OF RAGE INHIBITORS 1–19: BINDING TO THE EXTRACELLULAR DOMAIN

This section considers RAGE as a therapeutic target and discusses synthetic small-molecule inhibitors that have been developed to date.

The [3-(4-{2-butyl-1-[4-(4-chlorophenoxy)-phenyl]-1H-imidazole-4-yl}-phenoxy)-propyl]-diethylamine **1** (azeliragon, also called PF-04494700 or TTP488, Figure 3, Table 3) is an orally bioavailable small molecule able to cross the BBB.^{19,121,122} **1** inhibits the interaction between RAGE and A β _{1–42}, S100B, HMGB1, and CML. **1** also inhibits the binding of sRAGE to A β _{1–42} (IC₅₀ ~ 500 nM) determined by a fluorescent polarization assay.^{19,121,122}

In AD plaque-developing transgenic mice, the administration of **1** (ip 10 mg/kg per day or po 20 mg/kg per day) caused a significant reduction in inflammatory markers (TNF- α , TGF- β , and IL-1), CNS amyloid deposition and improvement of cognitive functions.¹⁹ **1** reduced accumulation of A β peptides in

the spleen and the expression of IL-6 and macrophage colony stimulating factor in a mouse model of systemic amyloidosis.¹²²

The safety and efficacy of **1** has been investigated in humans (phase I and II clinical trials).^{19,121,122} In the double-blind phase IIa trial, mild-to-moderate AD patients were treated orally with high dose of **1** (27 patients with 60 mg/day for 6 days then 20 mg daily for up to 10 weeks), low dose (28 patients with 30 mg/day for 6 days then 10 mg daily for up to 10 weeks), or placebo (12 patients). The doses appeared to be safe and well tolerated, but treatment did not show any differences in plasma A β levels, inflammatory biomarkers, or cognitive measures.¹²² A larger multicenter study involving 399 AD patients (phase II trial, NCT00566397) was carried out to determine if there was any evidence of **1**'s efficacy in slowing down cognitive decline: 135 patients were assigned to a high dose of **1** (60 mg/day for 6 days followed by 20 mg/day for up to 6 months), 135 patients to a lower dose (20 mg/day for 6 days followed by 5 mg/day for up to 18 months), and 132 participants to placebo.¹⁹ The high dose treatment was discontinued at 6 months due to confusion, falls, and significant worsening in cognitive measures (no changes to CSF and plasma levels of A β were observed). The accelerated cognitive decline slowed post treatment.¹⁹ In contrast, patients treated with the lower dose showed a beneficial effect against cognitive decline.¹²¹ The phase III clinical trial of RAGE inhibitor **1** is currently in progress in a mild AD cohort (2015–2018, NCT02080364, ClinicalTrials.gov).

The structure of **1** presents two hydrophobic moieties, an aliphatic chain and an electron deficient aromatic group, attached to a heteroaromatic central core (Figure 3). The central core is linked to an alkyl chain containing a protonable nitrogen. By substituting the imidazole ring with a thiazole, a library of RAGE antagonists was synthesized and evaluated, leading to the discovery of the trisubstituted thiazole **2** (Figure 3, Table 3) able to inhibit the RAGE-A β _{1–42} interaction (IC₅₀ = 1.21 μ M).¹²³ Structure–activity relationship (SAR) studies revealed that the aminoalkoxy linker is essential for RAGE inhibition, and no significant differences in inhibitory activity are observed by modifying the thiazole ring or by inserting an amide or an amino group between the thiazole and the 4-chlorophenoxyphenyl. Using an artificial BBB system, **2** showed A β transport inhibition using a RAGE-overexpressing brain endothelial cells monolayer.¹²³

Similarities with the pharmacophore of **1,2** are observed in a new class of 4,6-diaryl 2-aminopyrimidines (**3–6**, Figure 3), which exhibited good inhibitory activities against RAGE-A β interaction in an enzyme-linked immunosorbent assay (ELISA, IC₅₀ values <20 μ M).^{124–126} Inhibitors **3–6** comprise two aromatic groups (4-halophenyl ring), a pyrimidine central core and an alkyl chain containing a protonable nitrogen. SPR showed that **3** directly binds to RAGE (K_d = 102 μ M).¹²⁴ The binding mode of **3** to the RAGE V domain was evaluated through a flexible computational docking study, showing that **3** forms a net of hydrogen bonds between: (a) the oxygen atom of the ethoxy linker and Arg48, (b) two nitrogen atoms of the pyrimidine core and Arg104, and (c) the terminal amine and Met102.¹²⁴ Moreover, the two electronegative 4-chlorophenyl rings interact with a positively charged area rich in Lys and Arg residues.¹²⁴ In vitro studies showed that **3** (10 μ M) causes a down-regulation of A β -induced NF- κ B signaling in C6 glioma cells.¹²⁴ However, **3** exhibited high toxicity when administered to hippocampal neuronal cells (HT22) at 10 μ M (cell survival: 37.3%).¹²⁵ In vivo studies in wild-type mice showed that **3**

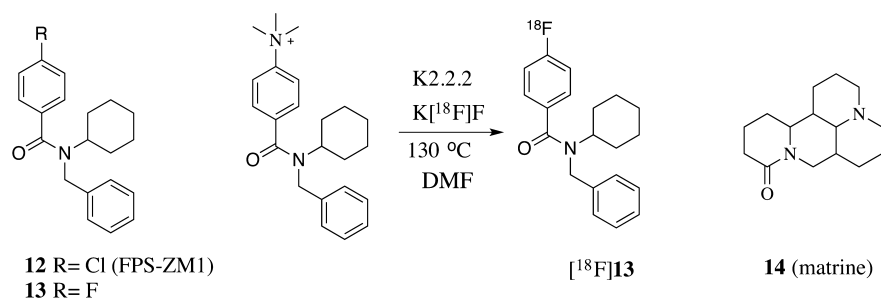


Figure 4. Structures of 12–14 and radiosynthesis of [^{18}F]13.

injected (ip) prior to human $A\beta$ administration inhibited $A\beta$ brain entry via RAGE at the BBB.¹²⁴ Oral administration of 3 (50 mg/kg per day for up to three months) to APPsw/PS1 mice significantly lowered the concentration of toxic soluble $A\beta$ in the brain and improved cognitive function.¹²⁴ Again, SAR studies highlighted that the *N*-aryl linker is crucial for RAGE inhibition, and its modification might lead to loss of biological activity.

Modifications on the position of the *N,N*-diethylamino linker of the aromatic ring led to improvements in potency of 2-aminopyrimidine derivative 4 ($\text{IC}_{50} = 4.6 \mu\text{M}$).¹²⁴ Further modifications to the terminal tertiary amine unit and linker length led to the discovery of 5 (Figure 3). The flexibility of the *N,N*-diethylamino linker in 5 is restricted by using a pyrrolidine ring. 5 showed improved RAGE- $A\beta_{1-42}$ inhibition and solubility compared to 3.¹²⁶ The binding mode, predicted by molecular docking, of 5 is similar to 3, however, additional hydrogen bonds are predicted to occur between Arg48 and the nitrogen atom of the pyrrolidine ring. In addition, the dimethylamino group attached to the pyrrolidine ring lies in a relatively hydrophobic section consisting of Met102 and Gly106.¹²⁶

Hence, a pyrimidine-2-carboxamide analogue 6 (Figure 3) was designed by replacing the chlorine with fluorine atom and by inserting an amide group in the central core.¹²⁵ 6 showed low cytotoxicity (100.4 \pm 3.2% of cell viability with HT22 cells) and superior RAGE inhibition than 3 at 20 μM (ELISA assay).¹²⁵

By substituting the pyrimidine ring of 6 with a pyrazole ring, Han et al. synthesized a library pyrazole-5-carboxamide derivatives.¹²⁷ Among them, 7 (Figure 3), containing a fluorobenzene, a butoxy substituent, and the essential *N,N*-(diethyl)phenoxyalkylamine moiety, showed better RAGE inhibitory activity ($\text{IC}_{50} = 1.9 \mu\text{M}$, ELISA) than 3 ($\text{IC}_{50} = 16.5 \mu\text{M}$).¹²⁷ SPR assays confirmed their direct binding to RAGE (K_d (7) = 43.4 μM , K_d (3) = 102 μM).¹²⁷ Analogues of 7 that do not contain the butoxy substituent maintained good RAGE inhibitor activity. Molecular docking analysis of 7 using the RAGE V domain suggested that the 4-fluorophenyl moiety might fit into an electropositive groove formed by Lys107.¹²⁷ Undesired cytotoxicity was observed in HT22 cells at 10 μM (cell survival: 10.3%).¹²⁵ In vivo studies of 7 (iv 25 mg/kg) in wild-type mice prior to iv human $A\beta$ administration showed that 7 is able to reduce $A\beta$ entry in the brain.¹²⁷

A series of benzoxazole analogues reported by Lee et al. have a similar pharmacophore: an electron deficient aromatic group, a heteroaromatic central core, and a linker containing a protonable nitrogen.

The interaction between RAGE and $A\beta$ was measured by a fluorescence resonance energy transfer (FRET) assay on mouse HT22 cells using RAGE-cyanine dye and $A\beta$ -fluorescein. The

reduction of the FRET signal induced by a library of benzoxazole analogues (4 μM) was recorded and calculated as percentage of inhibition. A 6-phenoxy-2-phenylbenzoxazole derivative 8 (Figure 3) inhibited the RAGE- $A\beta$ interaction in vitro (65%) and was not toxic in HT22 cells at 10 μM .¹²⁸ SAR studies demonstrated how the substitution of the chloride on the electron deficient aromatic group with a fluorine or CF_3 did not improve the activity. Instead, compounds with a long and flexible linker showed good RAGE inhibition.¹²⁸ Modification of the basicity of the nitrogen atom was deleterious to biological activity.¹²⁸ Administration of 8 (po 50 mg/kg every 2 days for 4 weeks) to transgenic APPsw/PS1 mice (34 weeks old) blocked the transport of peripheral $A\beta_{1-40}$ into the brain but did not significantly affect $A\beta$ and amyloid plaque levels in the brain.¹²⁸

Compounds 9–11 (Figure 3), having similar chemical features to 1–8, were able to inhibit the interaction of sRAGE to S110B (IC_{50} of 1.75, <0.5, and <0.5 μM , respectively), amyloid β (3.4, <0.5, and <0.5 μM , respectively) and CML (2.29, <0.5, and <0.5 μM , respectively).^{129–132}

N-Benzyl-*N*-cyclohexyl-4-chlorobenzamide 12 (FPS-ZM1, Figure 4) was selected through screening 5000 compounds in the search for RAGE inhibitors.¹⁷ 12 appeared to block the interaction between $A\beta_{1-40}$ and $A\beta_{1-42}$ and RAGE V domain in vitro and in vivo.¹⁷ Using a cell-free assay with immobilized sRAGE, 12 blocked RAGE binding to $A\beta$ ($K_i = 25 \text{ nM}$), S100B ($K_i = 230 \text{ nM}$), and HMGB1 ($K_i = 148 \text{ nM}$) and did not bind to immobilized $A\beta$.¹⁷ The SAR of 12 revealed that the features associated with RAGE binding are (1) a tertiary amide central core, (2) an electron deficient benzene, (3) a hydrophobic moiety, and (4) an electron-rich benzene ring linked to the amide with an alkyl spacer.¹³³ The binding mode of 13 (Figure 4), a fluorine analogue of 12, to the RAGE V domain was predicted by molecular docking studies.¹⁸ This binding appeared to be largely dependent on hydrophobic interactions with Pro45, Leu49, Trp51, Pro66, Leu78, and Pro80.¹⁸

In a receptor-binding assay using RAGE-transfected Chinese hamster ovary (CHO) cells, 12 inhibited the RAGE- $A\beta$ interaction with a K_i of 25 nM.¹⁷ In RAGE-transfected CHO cells, 12 was nontoxic at 10 μM and reduced RAGE-mediated cellular oxidative stress, BACE1 mRNA, BACE1 activity (induced by $A\beta_{1-40}$ and $A\beta_{1-42}$), and nuclear NF- κB levels (induced by $A\beta_{1-40}$).¹⁷

In 15–17-month-old APPsw/0 mice, 12 was not toxic up to 500 mg/kg (ip) and inhibited RAGE-mediated influx of circulating $A\beta_{1-40}$ and $A\beta_{1-42}$ into the brain at the luminal side of BBB, reducing their levels in the cortex and the hippocampus. Furthermore, 12 bound exclusively to RAGE in the CNS. The treatment with 12 (ip 1 mg/kg daily for 2 months) also reduced soluble APP β protein, p65, NF- κB , and

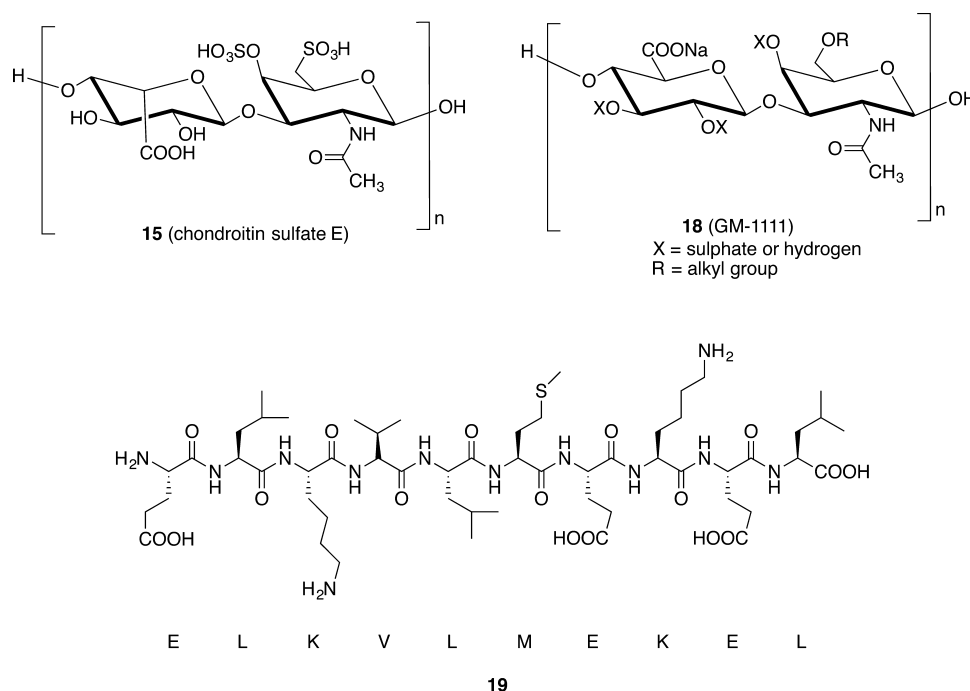


Figure 5. Structures of glycosaminoglycans (**15** and **18**) and the small peptide **19**.

BACE1 mRNA levels in the cortex and the hippocampus. As a result, **12** reduced $A\beta$ -induced RAGE-dependent oxidative stress in neurons, suppressed microglia activation, and neuroinflammation as well as normalized cerebral blood flow and cognitive performance.¹⁷

A RAGE-AGEs rat model, activated by intrahippocampal injection of AGEs, treated with **12** (ip 1 mg/kg/day for 4 weeks), showed a reduction of: (1) expression of $A\beta$ and amyloid precursor protein (APP) production, (2) NF- κ B-mediated $A\beta$ production, (3) inflammatory response in the cortex and hippocampus, and (4) ROS and lipid peroxidation along with an increased antioxidant enzyme activity.⁴⁶ In the aortas of aged rats, **12** reduced malondialdehyde and ROS production and increased GSH/GSSG ratio.¹³⁴

Fluorine-18 radiolabeled **13** ($[^{18}\text{F}]\mathbf{13}$, Figure 4) was developed for use in positron emission tomography (PET) imaging in vivo.¹⁸ $[^{18}\text{F}]\mathbf{13}$ was obtained using a trimethylammonium precursor and $[^{18}\text{F}]\text{fluoride}$ in the presence of Kryptofix-2.2.2 (K2.2.2) in DMF at 130 °C for 30 min.¹⁸ In vitro autoradiography of human brain tissue showed higher uptake of $[^{18}\text{F}]\mathbf{13}$ in the frontal cortex of AD compared with healthy control tissue. However, when studied in vivo, significant nonspecific binding to the white matter was observed, peaking within 3 min post iv injection and followed by virtually complete washout over the duration of the PET scan. $[^{18}\text{F}]\mathbf{13}$ was rapidly metabolized in rat liver microsomes.¹⁸

The RAGE inhibitor **14** (matrine, Figure 4) was identified by high-throughput screening of the main components of Chinese traditional medicinal herbs.¹³⁵ **14** suppressed the $A\beta$ -mediated RAGE signaling pathway in vitro and in vivo. However, microscale thermophoresis studies revealed a weak interaction between **14** and RAGE. Docking simulations proposed that **14** interacts with V domain through hydrogen bonding and a hydrophobic interaction with Ile26, Leu34, Val35, Leu36, and Lys37.¹³⁵ Aggregation studies using ThT fluorescence and TEM microscopy showed that **14** (50 μM) prevents $A\beta$ aggregation or fibrillation. In RAGE-overexpressing neuro-

blastoma cell lines, **14** (50 μM) inhibits the $A\beta_{1-42}$ aggregation and suppresses the RAGE- $A\beta$ signaling pathway, as demonstrated by the decrease of NF- κ B and BACE1 expression levels. In AD transgenic mice model studies, **14** (ip 100 mg/kg) is transported across the BBB, reduces brain $A\beta$, NF- κ B, BACE1 levels, and downregulates proinflammatory cytokines (TNF- α and IL-1 β) as well as attenuates memory deficits.¹³⁵

Glycosaminoglycans **15** (chondroitin sulfate E, Figure 5), **16** (heparan sulfate), and **17** (heparin) have a high affinity for RAGE ($K_d = 0.2, 0.6,$ and 3.1 nM, respectively).^{136,137} A single preadministration of **15** or **16** suppressed the colonization of the lungs by cancer cells.^{136,137} The antagonistic effect of **17** against RAGE inhibited tumor cell growth, migration, invasion, and distant metastasis in vitro and in vivo.⁴⁸ A non-anticoagulant semisynthetic glycosaminoglycan ether with an average molecular weight of 5.5 kDa **18** (GM-1111, Figure 5) exhibited a RAGE binding affinity of 1.69 nM.¹³⁷ **18** inhibited the interaction of RAGE with CML, S100B, and HMGB-1 with IC₅₀ values of 413, 275, and 80 nM, respectively. The acidic anionic and alkyl groups of **18** are likely to interact with the V domain containing hydrophobic and basic amino acids.¹³⁷ Furthermore, **18** displayed a substantial anti-inflammatory activity at nanomolar concentrations.¹³⁷

Two studies on RAGE antagonistic peptides have been reported so far. Peptide **19** (ELKVLMEKEL, Figure 5), developed from the structure of S100P, competes for a site on RAGE that is required for receptor binding by S100P, S100A4, and HMGB.¹³⁸ **19** reduced RAGE activation of NF- κ B, inflammation, tumor growth, and metastasis in several cancer cell lines. Using immune-deficient mice implanted with cancer cells, ip delivery of **19** caused a reduction of tumor growth, metastasis, and inflammation.¹³⁸ Peptides derived from the carboxy-terminal region of HMGB1 (150–183, 162–177, and 160–183) bind to RAGE and efficiently inhibit RAGE–HMGB1 mediated invasive migration of tumor cells both in vitro and in vivo.⁶³

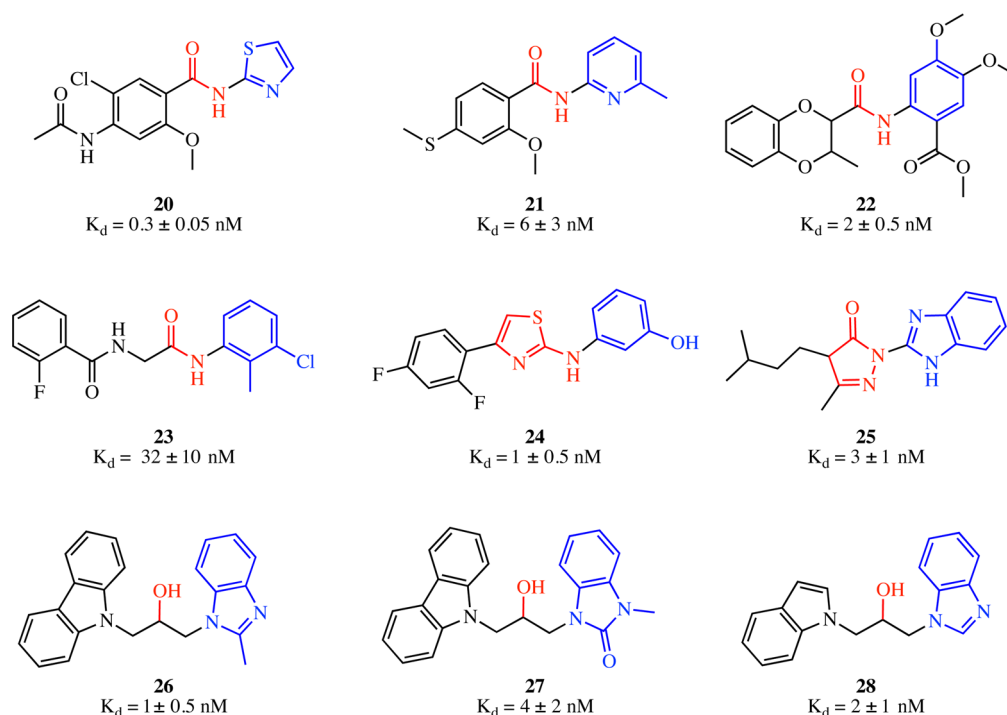


Figure 6. Small organic molecules binding the cytoplasmic domain of RAGE.

RAGE INHIBITORS BINDING TO THE INTRACELLULAR RAGE DOMAIN (20–28)

A novel mechanism for specific inhibition of RAGE signaling has been proposed by using inhibitors targeting the cytoplasmic domain of RAGE interfering with the RAGE–DIAPH1 interaction. A library of 58000 small molecules were evaluated by a high throughput RAGE–DIAPH1 binding assay.³⁵ Fluorescence titration experiments and NMR spectroscopy demonstrated that compounds 20–28 (Figure 6, Table 3) exhibited nM affinity ($K_d = 0.3$ –32 nM) to the cytoplasmic domain of RAGE responsible for RAGE–DIAPH1 interaction.^{35,139}

20–25 present a common pharmacophore, which can be divided in three different moieties: (1) a hydrophobic aromatic or aliphatic moiety (in black), (2) a central group that may form hydrogen bonds (in red), and (3) a substituted aromatic/heteroaromatic moiety (in blue). The other set of compounds 26–28 contain a hydrophobic tricyclic ring and a benzimidazole connected by an alkyl chain bearing an hydroxyl group, thereby ensuring the possibility of donating and accepting hydrogen bonds. NMR spectroscopy demonstrated that 20–28 interact with the cytoplasmic domain of RAGE by forming hydrogen bonds with Gln364 and Gln367 and a cation– π interaction with Arg365 and Arg366.³⁴ However, the binding sites of compounds 20–25 and 26–28 may not completely overlap.³⁴

In vitro RAGE–DIAPH1 competitive inhibitors displayed inhibitory effects on RAGE–CML signal transduction, vascular cell migration, and pro-inflammatory cytokines. In vivo RAGE–DIAPH1 inhibitors decreased inflammation caused by CML or methylated bovine serum albumin on wild-type mice.^{35,139}

FUTURE PERSPECTIVE AND CONCLUSIONS

This perspective reviews the state-of-the-art regarding: (1) the endogenous intracellular RAGE ligands and extracellular

effectors, and biochemical pathways modulated by the activation of RAGE, (2) the small molecule RAGE inhibitors and SAR generated to date, and (3) the use of RAGE inhibitors for potential treatment of cancer, cardiovascular diseases, and neurodegeneration.

Well-defined binding models have been developed for many RAGE–ligand interactions (AGEs, S100A6, S100B, S100P, and DIAPH1), however, relatively little is known about the binding sites of quinolinic acid, HMGB1, S100A12, $\alpha\beta$, or intracellular effector proteins, including TIRAP, ERK, PKC ξ , and DOCK7.^{22,24,28,34,62,72,83,87,140}

All studies investigating the binding of RAGE to its intracellular effector proteins have employed different cell lines and have not unequivocally established the phosphorylation status of Ser391 upon ligand binding to the extracellular domain, hampering a clear interpretation of data obtained.^{33–36,89} While TIRAP requires phosphorylation of RAGE for its interaction, ERK binds to both phosphorylated and unphosphorylated RAGE.^{33,36} The significance of the phosphorylation status of other intracellular effectors is still unknown. The question of whether or not simultaneous binding of multiple ligands/effectors to RAGE is required to initiate the downstream signaling also remains unanswered. Further crystallography, NMR, and computational studies are required to clarify precise binding mechanisms of intracellular effectors to the cytoplasmic RAGE domain.

Some of the mechanistic questions posed above may be addressed by exploring the changes in the expression of signaling genes (e.g., JNK, AKT, Cdc42, NF- κ B) following the inhibition of each extracellular or intracellular RAGE–ligand interaction in different cellular models. This may not only lead to improved understanding of differences in RAGE signaling pathways in each disease state (potentially identifying new molecular targets) but would also help design more disease-specific inhibitors.

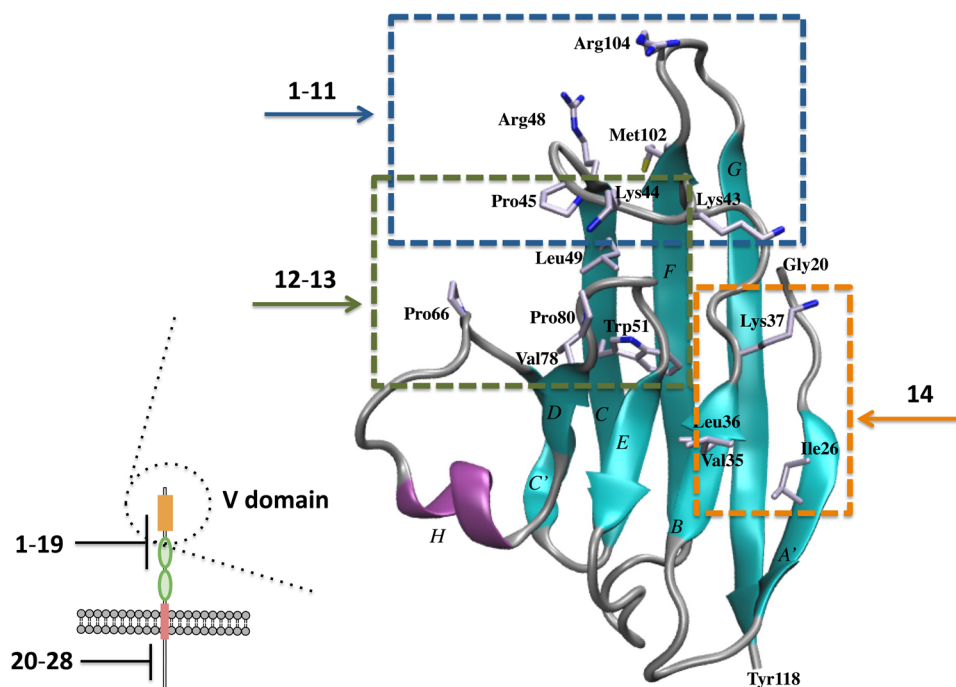


Figure 7. A cartoon of the V domain structure of the human RAGE with putative binding sites of 1–14 (dashed lines) is depicted. 1–19 bind to the V domain and 20–28 to the cytoplasmic region.

Another variable to consider is the degree of RAGE oligomerization.^{21,23,28–30} Small molecules which inhibit/stabilize this process may prove effective by reducing the RAGE–ligand interaction and preventing the downstream effects (e.g., activation of intracellular effectors, GTPase, or kinase-mediated pathways).

All truncated isoforms of RAGE (sRAGE, DN-RAGE, N-RAGE) occur naturally in tissues but do not trigger intracellular downstream signaling. Among them, sRAGE has been investigated as a disease biomarker and scavenger of excessive AGE, S100, HMGB1, or $A\beta$, thus decreasing their accumulation at the site of organ damage.^{11,13,14,56} Similarly, small molecules which enhance the level of truncated isoforms of RAGE at the expense of full-length RAGE may act as modulators of RAGE-mediated pathophysiological processes.

This review highlights a number of chemical entities that block RAGE activation by binding to the extracellular or intracellular domains.

Potent and selective inhibitors of RAGE (1–19) binding to three regions of V domain have been discovered and developed. Compounds 1–11 were found to possess activity in cell-based assays and in AD animal models, with the most advanced compound 1 undergoing clinical trials in patients with mild AD.^{19,122–127} These compounds share a common pharmacophore: one or two hydrophobic aromatic rings, a central core with hydrogen bond acceptor/donor atoms, and a alkyl linker bearing a protonable amine. It has been proposed by docking simulation that they interact with a pocket consisting of Lys43, Lys44, Arg48, Met102, and Arg104 (Figure 7).

The RAGE-specific inhibitor 12 has the ability to disrupt RAGE– $A\beta_{1-40}$ interactions, exhibits acceptable BBB permeability, and has a good toxicology profile in cell culture and rodents.^{17,46} Compound 12 also reduces amyloid- β -mediated brain dysfunction in murine models of AD.^{17,46} 12 was used as a chemotype for development of the potential PET radiotracer ($[^{18}\text{F}]13$) with the aim to quantify CNS RAGE in vivo.¹⁸

Further in vivo characterization of this radiotracer will be required to demonstrate the potential utility of $[^{18}\text{F}]13$. Molecular docking studies of RAGE protein confirmed that the interaction of 12,13 with its conserved residues (Leu49 and Trp51, Figure 7) is important for the RAGE– $A\beta$ interaction.¹⁴⁰

Compound 14 inhibits $A\beta$ -induced cytotoxicity and suppresses the RAGE– $A\beta$ signaling pathway in vitro and in vivo.¹³⁵ 14 reduces proinflammatory cytokines and $A\beta$ deposition, attenuating the memory deficits of AD transgenic mice.¹³⁵ Molecular docking analysis of 14 demonstrated its binding pattern to the V domain through hydrophobic interactions with Val35, Leu36, and Ile26 as well as hydrogen bonds with Lys37 (Figure 7).¹³⁵ However, the three binding regions of 1–14 involved in the interaction with RAGE have been proposed solely based on molecular docking simulations (Figure 7). Therefore, the elucidation of structures of RAGE–inhibitor complexes by X-ray or NMR should confirm the proposed binding mode and provide useful tools for future design of more stable and/or potent inhibitors. By binding to the extracellular domain of RAGE, glycosaminoglycans (15–18)^{136,137} and the small peptide (19)¹³⁸ inhibited tumor cell growth, migration, invasion, and metastasis in vitro and in vivo.

Manigrasso et al. identified 20–28 as potent RAGE inhibitors binding to the intracellular domain (Figure 7). They exhibit in vitro and in vivo inhibition of RAGE-dependent molecular processes.³⁵ NMR spectroscopy studies demonstrated that 20–28 interacted directly with the domain involved in the DIAPH1 interaction. This domain is not present in the truncated isoforms of RAGE (sRAGE and DN-RAGE), and therefore offers great promise for the future development of RAGE inhibitors specific for the full length RAGE.

The intracellular (1–19) and extracellular (20–28) inhibitors discussed above may act as scaffolds for further chemical refinement and optimization tailoring their activity, selectivity, and pharmacokinetics and leading to future success in the development of in vivo imaging radiotracers. Such tracers

would help elucidate the changes of *in vivo* RAGE expression and distribution in both normophysiological and pathological conditions.

The results obtained by *in vitro* and *in vivo* studies of **1–28** confirmed how RAGE inhibition could be a powerful tool for the management of immunoinflammatory pathologies. Independent of the physiological model used, the inhibition of RAGE resulted in a normalized inflammatory response as evidenced by the reduction in NF- κ B activation, cytokine production, and RAGE expression. Given the crucial role of RAGE in many diseases, it is anticipated that these initial chemical scaffolds will prime RAGE drug discovery programs in the field of neurodegeneration, tumorigenesis, and vascular disease. The diversity of RAGE signaling, activated through the binding of various ligands and effectors, suggests that future research should consider the affinity of RAGE inhibitors for different RAGE domains, oligomers, and isoforms. In addition, compounds targeting downstream proteins could provide a desired synergistic effect once combined with a RAGE inhibitor. The existing RAGE-specific molecules may serve as useful scaffolds for future ligand-based development and optimization of novel drug candidates targeting RAGE. Further developments in the characterization of 3D RAGE–inhibitor complexes will be crucial for the generation of new RAGE chemotypes and “drug-like” molecules using a structure-based drug design approach. Given the emerging importance of this target in multiple diseases, future developments in RAGE medicinal chemistry presents fertile ground for the development of a new generation of novel therapeutics.

■ AUTHOR INFORMATION

Corresponding Author

*Phone: +44 (0)20 718 88376. Fax: +44 (0)20 718 83056. E-mail: salvatore.bongarzone@kcl.ac.uk.

ORCID

Antony D. Gee: [0000-0001-8389-9012](https://orcid.org/0000-0001-8389-9012)

Notes

The authors declare no competing financial interest.

Biographies

Salvatore Bongarzone is a Postdoctoral Research Associate at the Division of Imaging Sciences and Biomedical Engineering, King's College London under the mentorship of Profs. Antony D. Gee and Federico Turkheimer. His active research focuses on developing carbon-11 and fluorine-18 PET radiotracers. He received his Ph.D. in Physics and Chemistry of Biological Systems (2011) from the International School of Advanced Studies (SISSA/ISAS) Trieste, Italy, under the supervision of Profs. P. Carloni, G. Legname, and M. L. Bolognesi. During his doctoral studies, Salvatore developed multitarget directed ligands against neurodegenerative prion diseases. In November 2013, he completed a postdoctoral research fellowship at the Institute of Research in Biomedicine (IRB), Barcelona, Spain, cofunded by EU MarieCurie Actions working in the groups of Profs. F. Albericio and M. Coll. He developed small molecule inhibitors against UL89 cytomegalovirus terminase, which is involved in viral replication, combining *in silico* modelling, X-ray crystallography, and *in vitro* studies.

Vilius Savickas is currently pursuing a Master's degree in Clinical Research at King's College London/National Institute for Health Research Biomedical Research Centre at Guy's and St. Thomas' NHS Foundation Trust under Prof. Antony Gee's and Dr. Salvatore Bongarzone's supervision. His research project focuses on the *ex vivo* and *in vivo* development of novel PET imaging agents for Alzheimer's

disease utilizing a centrally acting RAGE inhibitor. Vilius had previously obtained a Master of Pharmacy degree at Kingston University, London, during which he investigated the cytotoxic effects of naturally occurring polyphenol compounds in colorectal cancer cell lines. His current research interests lie in translational neuropharmacology and clinical education.

Federico Luzi is now working on his Master's thesis in Medicinal Chemistry and Pharmaceutical Technology at King's College London/National Institute for Health Research Biomedical Research Centre at Guy's and St. Thomas' NHS Foundation Trust under Prof. Antony Gee's and Dr. Salvatore Bongarzone's supervision. His study focuses on the chemical development of a novel radiotracer for PET imaging able to highlight early stages of Alzheimer's disease. Previous studies have been carried at Alma Mater Studiorum, University of Bologna, Italy, and University of California, Irvine, USA, where he specialized in neurosciences and medicinal chemistry.

Antony D. Gee is Professor of PET and Radiochemistry in the Division of Imaging Sciences at King's College London. He obtained a B.Sc.(Hons) in Chemistry at the University of Sussex (1985), and his Ph.D. in Radiopharmaceutical Organic Chemistry at Uppsala University, Sweden (1991). Since then he has worked as the Director of PET Chemistry at the Guy's and St. Thomas' Hospitals Clinical PET Centre, UMDS, London, and the Aarhus University Hospital PET Centre in Aarhus, Denmark, before moving to GlaxoSmithKline to spearhead the use of PET imaging in drug discovery and development. A number of very active research projects are in progress including the development of rapid labelling synthetic techniques with short-lived positron-emitting radionuclides, the design of PET imaging probes, and the understanding of *in vivo* pharmacology.

■ ACKNOWLEDGMENTS

This work was supported by Medical Research Council (MRC, MR/K022733/1) and European Commission, FP7-PEOPLE-2012-ITN (316882, RADIOMI). We acknowledge financial support from the Department of Health via the National Institute for Health Research (NIHR) Biomedical Research Centre at Guy's & St. Thomas' NHS Foundation Trust and King's College London and the Centre of Excellence in Medical Engineering funded by the Wellcome Trust and EPSRC under grant no. WT 088641/Z/09/Z.

■ ABBREVIATIONS USED

AP-1, activator protein 1; AGE, advanced glycation endproduct; AD, Alzheimer's disease; A β , amyloid beta; AKT, protein kinase B; BBB, blood–brain barrier; Cdc42, cell division control protein 42 homologue; CNS, central nervous system; CHO, chinese hamster ovary cell; DOCK7, dedicator of cytokinesis 7; DIAPH1, diaphanous-related formin 1; DN-RAGE, dominant negative RAGE; ELISA, enzyme-linked immunosorbent assay; ERK, extracellular signal-regulated kinases; FRET, fluorescence resonance energy transfer; HMGB1, high mobility group box 1; MG, methylglyoxal; MAPK, mitogen-activated protein kinase; MEK, mitogen-activated protein kinase kinase; MYD88, myeloid differentiation primary response gene 88; MG-H1, methylglyoxal-derived hydroimidazolone-1; CML, *N* ϵ -carboxymethyl-lysine; CEL, *N* ϵ -carboxy-ethyl-lysine; N-RAGE, N-truncated RAGE; ITC, isothermal titration calorimetry; MMP, metalloproteinase; NF- κ B, nuclear factor kappa-light-chain-enhancer of activated B cells; NMR, nuclear magnetic resonance; PET, positron emission tomography; PKC ξ , protein kinase C ξ ; RAGE, receptor for advanced glycation end-

products; sRAGE, soluble/secretory RAGE; ROS, reactive oxygen species; BACE1, β -site amyloid precursor protein cleaving enzyme 1; SAR, structure-activity relationship; SPR, surface plasmon resonance; TIRAP, toll-interleukin 1 receptor domain containing adaptor protein; TLR, toll-like receptor

REFERENCES

- (1) Vistoli, G.; De Maddis, D.; Cipak, A.; Zarkovic, N.; Carini, M.; Aldini, G. Advanced glycooxidation and lipoxidation end products (AGEs and ALEs): an overview of their mechanisms of formation. *Free Radical Res.* **2013**, *47* (Sup 1), 3–27.
- (2) Adrover, M.; Marino, L.; Sanchis, P.; Pauwels, K.; Kraan, Y.; Lebrun, P.; Vilanova, B.; Munoz, F.; Broersen, K.; Donoso, J. Mechanistic insights in glycation-induced protein aggregation. *Biomacromolecules* **2014**, *15*, 3449–3462.
- (3) Sajithlal, G. B.; Chithra, P.; Chandrakasan, G. Advanced glycation end products induce crosslinking of collagen in vitro. *Biochim. Biophys. Acta, Mol. Basis Dis.* **1998**, *1407*, 215–224.
- (4) Nenna, A.; Spadaccio, C.; Lusini, M.; Ulianich, L.; Chello, M.; Nappi, F. Basic and Clinical Research Against Advanced Glycation End Products (AGEs): New Compounds to Tackle Cardiovascular Disease and Diabetic Complications. *Recent Pat. Cardiovasc. Drug Discovery* **2015**, *10*, 10–33.
- (5) Li, J.; Liu, D.; Sun, L.; Lu, Y.; Zhang, Z. Advanced glycation end products and neurodegenerative diseases: mechanisms and perspective. *J. Neurol. Sci.* **2012**, *317*, 1–5.
- (6) Rocken, C.; Kientsch-Engel, R.; Mansfeld, S.; Stix, B.; Stubenrauch, K.; Weigle, B.; Buhling, F.; Schwan, M.; Saeger, W. Advanced glycation end products and receptor for advanced glycation end products in AA amyloidosis. *Am. J. Pathol.* **2003**, *162*, 1213–1220.
- (7) Sparvero, L. J.; Asafu-Adjei, D.; Kang, R.; Tang, D.; Amin, N.; Im, J.; Rutledge, R.; Lin, B.; Amoscato, A. A.; Zeh, H. J.; Lotze, M. T. RAGE (Receptor for Advanced Glycation Endproducts), RAGE ligands, and their role in cancer and inflammation. *J. Transl. Med.* **2009**, *7*, 17.
- (8) Ramasamy, R.; Vannucci, S. J.; Yan, S. S. D.; Herold, K.; Yan, S. F.; Schmidt, A. M. Advanced glycation end products and RAGE: a common thread in aging, diabetes, neurodegeneration, and inflammation. *Glycobiology* **2005**, *15*, 16R–28R.
- (9) Ray, R.; Juranek, J. K.; Rai, V. RAGE axis in neuroinflammation, neurodegeneration and its emerging role in the pathogenesis of amyotrophic lateral sclerosis. *Neurosci. Biobehav. Rev.* **2016**, *62*, 48–55.
- (10) Neeper, M.; Schmidt, A. M.; Brett, J.; Yan, S. D.; Wang, F.; Pan, Y. C.; Elliston, K.; Stern, D.; Shaw, A. Cloning and expression of a cell surface receptor for advanced glycosylation end products of proteins. *J. Biol. Chem.* **1992**, *267*, 14998–15004.
- (11) Cheng, C.; Tsuneyama, K.; Kominami, R.; Shinohara, H.; Sakurai, S.; Yonekura, H.; Watanabe, T.; Takano, Y.; Yamamoto, H.; Yamamoto, Y. Expression profiling of endogenous secretory receptor for advanced glycation end products in human organs. *Mod. Pathol.* **2005**, *18*, 1385–1396.
- (12) Tanji, N.; Markowitz, G. S.; Fu, C.; Kislinger, T.; Taguchi, A.; Pischetsrieder, M.; Stern, D.; Schmidt, A. M.; D'Agati, V. D. Expression of advanced glycation end products and their cellular receptor RAGE in diabetic nephropathy and nondiabetic renal disease. *J. Am. Soc. Nephrol.* **2000**, *11*, 1656–1666.
- (13) Falcone, C.; Emanuele, E.; D'Angelo, A.; Buzzi, M. P.; Belvito, C.; Cuccia, M.; Geroldi, D. Plasma levels of soluble receptor for advanced glycation end products and coronary artery disease in nondiabetic men. *Arterioscler., Thromb., Vasc. Biol.* **2005**, *25*, 1032–1037.
- (14) Emanuele, E.; D'Angelo, A.; Tomaino, C.; Binetti, G.; Ghidoni, R.; Politi, P.; Bernardi, L.; Maletta, R.; Bruni, A. C.; Geroldi, D. Circulating levels of soluble receptor for advanced glycation end products in Alzheimer disease and vascular dementia. *Arch. Neurol.* **2005**, *62*, 1734–1736.
- (15) Riehl, A.; Nemeth, J.; Angel, P.; Hess, J. The receptor RAGE: Bridging inflammation and cancer. *Cell Commun. Signaling* **2009**, *7*, 12.
- (16) Nasser, M. W.; Wani, N. A.; Ahirwar, D. K.; Powell, C. A.; Ravi, J.; Elbaz, M.; Zhao, H.; Padilla, L.; Zhang, X.; Shilo, K.; Ostrowski, M.; Shapiro, C.; Carson, W. E., 3rd; Ganju, R. K. RAGE mediates S100A7-induced breast cancer growth and metastasis by modulating the tumor microenvironment. *Cancer Res.* **2015**, *75*, 974–985.
- (17) Deane, R.; Singh, I.; Sagare, A. P.; Bell, R. D.; Ross, N. T.; LaRue, B.; Love, R.; Perry, S.; Paquette, N.; Deane, R. J.; Thiyagarajan, M.; Zarcone, T.; Fritz, G.; Friedman, A. E.; Miller, B. L.; Zlokovic, B. V. A multimodal RAGE-specific inhibitor reduces amyloid beta-mediated brain disorder in a mouse model of Alzheimer disease. *J. Clin. Invest.* **2012**, *122*, 1377–1392.
- (18) Cary, B. P.; Brooks, A. F.; Fawaz, M. V.; Drake, L. R.; Desmond, T. J.; Sherman, P.; Quesada, C. A.; Scott, P. J. Synthesis and Evaluation of [(18F)RAGER: A First Generation Small-Molecule PET Radioligand Targeting the Receptor for Advanced Glycation Endproducts. *ACS Chem. Neurosci.* **2016**, *7*, 391–398.
- (19) Galasko, D.; Bell, J.; Mancuso, J. Y.; Kupiec, J. W.; Sabbagh, M. N.; van Dyck, C.; Thomas, R. G.; Aisen, P. S. Alzheimer's Disease Cooperative, S. Clinical trial of an inhibitor of RAGE-Abeta interactions in Alzheimer disease. *Neurology* **2014**, *82*, 1536–1542.
- (20) UniProtKB—Q15109 (RAGE_HUMAN); UniProt, 2017; <http://www.uniprot.org/uniprot/Q15109> (accessed April 6, 2017).
- (21) Yatime, L.; Andersen, G. R. Structural insights into the oligomerization mode of the human receptor for advanced glycation end-products. *FEBS J.* **2013**, *280*, 6556–6568.
- (22) Xue, J.; Rai, V.; Singer, D.; Chabierski, S.; Xie, J.; Reverdatto, S.; Burz, D. S.; Schmidt, A. M.; Hoffmann, R.; Shekhtman, A. Advanced glycation end product recognition by the receptor for AGEs. *Structure* **2011**, *19*, 722–732.
- (23) Koch, M.; Chitayat, S.; Dattilo, B. M.; Schiefner, A.; Diez, J.; Chazin, W. J.; Fritz, G. Structural basis for ligand recognition and activation of RAGE. *Structure* **2010**, *18*, 1342–1352.
- (24) Dattilo, B. M.; Fritz, G.; Leclerc, E.; vander Kooi, C. W.; Heizmann, C. W.; Chazin, W. J. The extracellular region of the receptor for advanced glycation end products is composed of two independent structural units. *Biochemistry* **2007**, *46*, 6957–6970.
- (25) Sturchler, E.; Galichet, A.; Weibel, M.; Leclerc, E.; Heizmann, C. W. Site-specific blockade of RAGE-Vd prevents amyloid-beta oligomer neurotoxicity. *J. Neurosci.* **2008**, *28*, 5149–5158.
- (26) Xue, J.; Ray, R.; Singer, D.; Bohme, D.; Burz, D. S.; Rai, V.; Hoffmann, R.; Shekhtman, A. The receptor for advanced glycation end products (RAGE) specifically recognizes methylglyoxal-derived AGEs. *Biochemistry* **2014**, *53*, 3327–3335.
- (27) Hori, O.; Brett, J.; Slattery, T.; Cao, R.; Zhang, J.; Chen, J. X.; Nagashima, M.; Lundh, E. R.; Vijay, S.; Nitecki, D.; et al. The receptor for advanced glycation end products (RAGE) is a cellular binding site for amphotericin. Mediation of neurite outgrowth and co-expression of RAGE and amphotericin in the developing nervous system. *J. Biol. Chem.* **1995**, *270*, 25752–25761.
- (28) Xie, J.; Reverdatto, S.; Frolov, A.; Hoffmann, R.; Burz, D. S.; Shekhtman, A. Structural basis for pattern recognition by the receptor for advanced glycation end products (RAGE). *J. Biol. Chem.* **2008**, *283*, 27255–27269.
- (29) Xie, J.; Burz, D. S.; He, W.; Bronstein, I. B.; Lednev, I.; Shekhtman, A. Hexameric calgranulin C (S100A12) binds to the receptor for advanced glycation end products (RAGE) using symmetric hydrophobic target-binding patches. *J. Biol. Chem.* **2007**, *282*, 4218–4231.
- (30) Zong, H.; Madden, A.; Ward, M.; Mooney, M. H.; Elliott, C. T.; Stitt, A. W. Homodimerization is essential for the receptor for advanced glycation end products (RAGE)-mediated signal transduction. *J. Biol. Chem.* **2010**, *285*, 23137–23146.
- (31) Xu, D.; Young, J. H.; Krahn, J. M.; Song, D.; Corbett, K. D.; Chazin, W. J.; Pedersen, L. C.; Esko, J. D. Stable RAGE-heparan sulfate complexes are essential for signal transduction. *ACS Chem. Biol.* **2013**, *8*, 1611–1620.
- (32) Rodriguez Gonzalez-Moro, J. M.; de Lucas Ramos, P.; Izquierdo Alonso, J. L.; Lopez-Muniz Ballesteros, B.; Anton Diaz, E.; Ribera, X.; Martin, A. Impact of COPD severity on physical disability and daily

living activities: EDIP-EPOC I and EDIP-EPOC II studies. *Int. J. Clin. Pract.* **2009**, *63*, 742–750.

(33) Sakaguchi, M.; Murata, H.; Yamamoto, K.; Ono, T.; Sakaguchi, Y.; Motoyama, A.; Hibino, T.; Kataoka, K.; Huh, N. H. TIRAP, an adaptor protein for TLR2/4, transduces a signal from RAGE phosphorylated upon ligand binding. *PLoS One* **2011**, *6*, e23132.

(34) Rai, V.; Maldonado, A. Y.; Burz, D. S.; Reverdatto, S.; Schmidt, A. M.; Shekhtman, A. Signal transduction in receptor for advanced glycation end products (RAGE): solution structure of C-terminal rage (ctRAGE) and its binding to mDia1. *J. Biol. Chem.* **2012**, *287*, 5133–5144.

(35) Manigrasso, M. B.; Pan, J.; Rai, V.; Zhang, J.; Reverdatto, S.; Quadri, N.; DeVita, R. J.; Ramasamy, R.; Shekhtman, A.; Schmidt, A. M. Small Molecule Inhibition of Ligand-Stimulated RAGE-DIAPH1 Signal Transduction. *Sci. Rep.* **2016**, *6*, 22450.

(36) Ishihara, K.; Tsutsumi, K.; Kawane, S.; Nakajima, M.; Kasaoka, T. The receptor for advanced glycation end-products (RAGE) directly binds to ERK by a D-domain-like docking site. *FEBS Lett.* **2003**, *550*, 107–113.

(37) Hudson, B. I.; Kalea, A. Z.; Del Mar Arriero, M.; Harja, E.; Boulanger, E.; D'Agati, V.; Schmidt, A. M. Interaction of the RAGE cytoplasmic domain with diaphanous-1 is required for ligand-stimulated cellular migration through activation of Rac1 and Cdc42. *J. Biol. Chem.* **2008**, *283*, 34457–34468.

(38) Huttunen, H. J.; Fages, C.; Rauvala, H. Receptor for advanced glycation end products (RAGE)-mediated neurite outgrowth and activation of NF-kappaB require the cytoplasmic domain of the receptor but different downstream signaling pathways. *J. Biol. Chem.* **1999**, *274*, 19919–19924.

(39) Harja, E.; Bu, D. X.; Hudson, B. I.; Chang, J. S.; Shen, X.; Hallam, K.; Kalea, A. Z.; Lu, Y.; Rosario, R. H.; Oruganti, S.; Nikolla, Z.; Belov, D.; Lalla, E.; Ramasamy, R.; Yan, S. F.; Schmidt, A. M. Vascular and inflammatory stresses mediate atherosclerosis via RAGE and its ligands in apoE^{-/-} mice. *J. Clin. Invest.* **2008**, *118*, 183–194.

(40) Jules, J.; Maiguel, D.; Hudson, B. I. Alternative splicing of the RAGE cytoplasmic domain regulates cell signaling and function. *PLoS One* **2013**, *8*, e78267.

(41) Zhang, L.; Bukulin, M.; Kojro, E.; Roth, A.; Metz, V. V.; Fahrenholz, F.; Nawroth, P. P.; Bierhaus, A.; Postina, R. Receptor for advanced glycation end products is subjected to protein ectodomain shedding by metalloproteinases. *J. Biol. Chem.* **2008**, *283*, 35507–35516.

(42) Pan, H.; He, L.; Wang, B.; Niu, W. The relationship between RAGE gene four common polymorphisms and breast cancer risk in northeastern Han Chinese. *Sci. Rep.* **2015**, *4*, 4355.

(43) Cai, W.; Li, J.; Xu, J. X.; Liu, Y.; Zhang, W.; Xiao, J. R.; Zhu, L. Y.; Liu, J. Y. Association of 2184AG Polymorphism in the RAGE Gene with Diabetic Nephropathy in Chinese Patients with Type 2 Diabetes. *J. Diabetes Res.* **2015**, *2015*, 310237.

(44) Hudson, B. I.; Carter, A. M.; Harja, E.; Kalea, A. Z.; Arriero, M.; Yang, H.; Grant, P. J.; Schmidt, A. M. Identification, classification, and expression of RAGE gene splice variants. *FASEB J.* **2008**, *22*, 1572–1580.

(45) Ding, Q.; Keller, J. N. Evaluation of rage isoforms, ligands, and signaling in the brain. *Biochim. Biophys. Acta, Mol. Cell Res.* **2005**, *1746*, 18–27.

(46) Hong, Y.; Shen, C.; Yin, Q.; Sun, M.; Ma, Y.; Liu, X. Effects of RAGE-Specific Inhibitor FPS-ZM1 on Amyloid-beta Metabolism and AGEs-Induced Inflammation and Oxidative Stress in Rat Hippocampus. *Neurochem. Res.* **2016**, *41*, 1192–1199.

(47) Kaji, Y.; Usui, T.; Ishida, S.; Yamashiro, K.; Moore, T. C.; Moore, J.; Yamamoto, Y.; Yamamoto, H.; Adamis, A. P. Inhibition of diabetic leukostasis and blood-retinal barrier breakdown with a soluble form of a receptor for advanced glycation end products. *Invest. Ophthalmol. Visual Sci.* **2007**, *48*, 858–865.

(48) Takeuchi, A.; Yamamoto, Y.; Munesue, S.; Harashima, A.; Watanabe, T.; Yonekura, H.; Yamamoto, H.; Tsuchiya, H. Low molecular weight heparin suppresses receptor for advanced glycation

end products-mediated expression of malignant phenotype in human fibrosarcoma cells. *Cancer Sci.* **2013**, *104*, 740–749.

(49) Li, Y.; Wu, R.; Tian, Y.; Yu, M.; Tang, Y.; Cheng, H.; Tian, Z. RAGE/NF-kappaB signaling mediates lipopolysaccharide induced acute lung injury in neonate rat model. *Int. J. Clin. Exp. Med.* **2015**, *8*, 13371–13376.

(50) Lue, L. F.; Walker, D. G.; Brachova, L.; Beach, T. G.; Rogers, J.; Schmidt, A. M.; Stern, D. M.; Yan, S. D. Involvement of microglial receptor for advanced glycation endproducts (RAGE) in Alzheimer's disease: Identification of a cellular activation mechanism. *Exp. Neurol.* **2001**, *171*, 29–45.

(51) Huang, J. S.; Guh, J. Y.; Chen, H. C.; Hung, W. C.; Lai, Y. H.; Chuang, L. Y. Role of receptor for advanced glycation end-product (RAGE) and the JAK/STAT-signaling pathway in AGE-induced collagen production in NRK-49F cells. *J. Cell. Biochem.* **2001**, *81*, 102–113.

(52) Reynolds, P. R.; Kasteler, S. D.; Cosio, M. G.; Sturrock, A.; Huecksteadt, T.; Hoidal, J. R. RAGE: developmental expression and positive feedback regulation by Egr-1 during cigarette smoke exposure in pulmonary epithelial cells. *Am. J. Physiol.: Lung Cell. Mol. Physiol.* **2008**, *294*, L1094–1101.

(53) Kosaka, T.; Fukui, R.; Matsui, M.; Kurosaka, Y.; Nishimura, H.; Tanabe, M.; Takakura, Y.; Iwai, K.; Waki, T.; Fujita, T. RAGE, receptor of advanced glycation endproducts, negatively regulates chondrocytes differentiation. *PLoS One* **2014**, *9*, e108819.

(54) Yonekura, H.; Yamamoto, Y.; Sakurai, S.; Petrova, R. G.; Abedin, M. J.; Li, H.; Yasui, K.; Takeuchi, M.; Makita, Z.; Takasawa, S.; Okamoto, H.; Watanabe, T.; Yamamoto, H. Novel splice variants of the receptor for advanced glycation end-products expressed in human vascular endothelial cells and pericytes, and their putative roles in diabetes-induced vascular injury. *Biochem. J.* **2003**, *370*, 1097–1109.

(55) Kalea, A. Z.; Schmidt, A. M.; Hudson, B. I. RAGE: a novel biological and genetic marker for vascular disease. *Clin. Sci.* **2009**, *116*, 621–637.

(56) Geroldi, D.; Falcone, C.; Emanuele, E. Soluble receptor for advanced glycation end products: from disease marker to potential therapeutic target. *Curr. Med. Chem.* **2006**, *13*, 1971–1978.

(57) Yamagishi, S.; Adachi, H.; Nakamura, K.; Matsui, T.; Jinnouchi, Y.; Takenaka, K.; Takeuchi, M.; Enomoto, M.; Furuki, K.; Hino, A.; Shiget, Y.; Imaizumi, T. Positive association between serum levels of advanced glycation end products and the soluble form of receptor for advanced glycation end products in nondiabetic subjects. *Metab., Clin. Exp.* **2006**, *55*, 1227–1231.

(58) Cho, H. J.; Son, S. M.; Jin, S. M.; Hong, H. S.; Shin, D. H.; Kim, S. J.; Huh, K.; Mook-Jung, I. RAGE regulates BACE1 and Abeta generation via NFAT1 activation in Alzheimer's disease animal model. *FASEB J.* **2009**, *23*, 2639–2649.

(59) Santilli, F.; Vazzana, N.; Bucciarelli, L. G.; Davi, G. Soluble forms of RAGE in human diseases: clinical and therapeutical implications. *Curr. Med. Chem.* **2009**, *16*, 940–952.

(60) Zhang, L.; Postina, R.; Wang, Y. Ectodomain shedding of the receptor for advanced glycation end products: a novel therapeutic target for Alzheimer's disease. *Cell. Mol. Life Sci.* **2009**, *66*, 3923–3935.

(61) Park, H.; Boyington, J. C. The 1.5 Å crystal structure of human receptor for advanced glycation endproducts (RAGE) ectodomains reveals unique features determining ligand binding. *J. Biol. Chem.* **2010**, *285*, 40762–40770.

(62) Ostendorp, T.; Leclerc, E.; Galichet, A.; Koch, M.; Demling, N.; Weigle, B.; Heizmann, C. W.; Kroneck, P. M.; Fritz, G. Structural and functional insights into RAGE activation by multimeric S100B. *EMBO J.* **2007**, *26*, 3868–3878.

(63) Huttunen, H. J.; Fages, C.; Kuja-Panula, J.; Ridley, A. J.; Rauvala, H. Receptor for advanced glycation end products-binding COOH-terminal motif of amphoterin inhibits invasive migration and metastasis. *Cancer Res.* **2002**, *62*, 4805–4811.

(64) Botos, I.; Segal, D. M.; Davies, D. R. The Structural Biology of Toll-like Receptors. *Structure* **2011**, *19*, 447–459.

(65) Sinha, P.; Okoro, C.; Foell, D.; Freeze, H. H.; Ostrand-Rosenberg, S.; Srikrishna, G. Proinflammatory S100 proteins regulate

the accumulation of myeloid-derived suppressor cells. *J. Immunol.* **2008**, *181*, 4666–4675.

(66) Rothermundt, M.; Peters, M.; Prehn, J. H.; Arolt, V. S100B in brain damage and neurodegeneration. *Microsc. Res. Tech.* **2003**, *60*, 614–632.

(67) Schlueter, C.; Weber, H.; Meyer, B.; Rogalla, P.; Roser, K.; Hauke, S.; Bullerdiek, J. Angiogenic signaling through hypoxia: HMGB1: an angiogenic switch molecule. *Am. J. Pathol.* **2005**, *166*, 1259–1263.

(68) Gao, T. L.; Yuan, X. T.; Yang, D.; Dai, H. L.; Wang, W. J.; Peng, X.; Shao, H. J.; Jin, Z. F.; Fu, Z. J. Expression of HMGB1 and RAGE in rat and human brains after traumatic brain injury. *J. Trauma Acute Care Surg.* **2012**, *72*, 643–649.

(69) Jara, N.; Leal, M. J.; Bunout, D.; Hirsch, S.; Barrera, G.; Leiva, L.; de la Maza, M. P. Dietary intake increases serum levels of carboxymethyl-lysine (CML) in diabetic patients. *Nutr. Hosp.* **2012**, *27*, 1272–1278.

(70) Berlanga, J.; Cibrian, D.; Guillen, I.; Freyre, F.; Alba, J. S.; Lopez-Saura, P.; Merino, N.; Aldama, A.; Quintela, A. M.; Triana, M. E.; Montequin, J. F.; Ajamieh, H.; Urquiza, D.; Ahmed, N.; Thornalley, P. J. Methylglyoxal administration induces diabetes-like microvascular changes and perturbs the healing process of cutaneous wounds. *Clin. Sci.* **2005**, *109*, 83–95.

(71) Leclerc, E.; Fritz, G.; Vetter, S. W.; Heizmann, C. W. Binding of S100 proteins to RAGE: an update. *Biochim. Biophys. Acta, Mol. Cell Res.* **2009**, *1793*, 993–1007.

(72) Leclerc, E.; Fritz, G.; Weibel, M.; Heizmann, C. W.; Galichet, A. S100B and S100A6 differentially modulate cell survival by interacting with distinct RAGE (receptor for advanced glycation end products) immunoglobulin domains. *J. Biol. Chem.* **2007**, *282*, 31317–31331.

(73) Onyeagucha, B. C.; Mercado-Pimentel, M. E.; Hutchison, J.; Flemington, E. K.; Nelson, M. A. S100P/RAGE signaling regulates microRNA-155 expression via AP-1 activation in colon cancer. *Exp. Cell Res.* **2013**, *319*, 2081–2090.

(74) Hofmann, M. A.; Drury, S.; Fu, C.; Qu, W.; Taguchi, A.; Lu, Y.; Avila, C.; Kambham, N.; Bierhaus, A.; Nawroth, P.; Neurath, M. F.; Slattey, T.; Beach, D.; McClary, J.; Nagashima, M.; Morser, J.; Stern, D.; Schmidt, A. M. RAGE mediates a novel proinflammatory axis: a central cell surface receptor for S100/calgranulin polypeptides. *Cell* **1999**, *97*, 889–901.

(75) Xue, J.; Manigrasso, M.; Scalabrin, M.; Rai, V.; Reverdatto, S.; Burz, D. S.; Fabris, D.; Schmidt, A. M.; Shekhtman, A. Change in the Molecular Dimension of a RAGE-Ligand Complex Triggers RAGE Signaling. *Structure* **2016**, *24*, 1509–1522.

(76) Mercado-Pimentel, M. E.; Onyeagucha, B. C.; Li, Q.; Pimentel, A. C.; Jandova, J.; Nelson, M. A. The S100P/RAGE signaling pathway regulates expression of microRNA-21 in colon cancer cells. *FEBS Lett.* **2015**, *589*, 2388–2393.

(77) Penumutchu, S. R.; Chou, R. H.; Yu, C. Structural insights into calcium-bound S100P and the V domain of the RAGE complex. *PLoS One* **2014**, *9*, e103947.

(78) Arumugam, T.; Simeone, D. M.; Schmidt, A. M.; Logsdon, C. D. S100P stimulates cell proliferation and survival via receptor for activated glycation end products (RAGE). *J. Biol. Chem.* **2004**, *279*, 5059–5065.

(79) Matsumoto, S.; Yoshida, T.; Murata, H.; Harada, S.; Fujita, N.; Nakamura, S.; Yamamoto, Y.; Watanabe, T.; Yonekura, H.; Yamamoto, H.; Ohkubo, T.; Kobayashi, Y. Solution structure of the variable-type domain of the receptor for advanced glycation end products: new insight into AGE-RAGE interaction. *Biochemistry* **2008**, *47*, 12299–12311.

(80) Kim, S.; Kim, S. Y.; Pribis, J. P.; Lotze, M.; Mollen, K. P.; Shapiro, R.; Loughran, P.; Scott, M. J.; Billiar, T. R. Signaling of high mobility group box 1 (HMGB1) through toll-like receptor 4 in macrophages requires CD14. *Mol. Med.* **2013**, *19*, 88–98.

(81) Orlova, V. V.; Choi, E. Y.; Xie, C.; Chavakis, E.; Bierhaus, A.; Ihanus, E.; Ballantyne, C. M.; Gahmberg, C. G.; Bianchi, M. E.; Nawroth, P. P.; Chavakis, T. A novel pathway of HMGB1-mediated

inflammatory cell recruitment that requires Mac-1-integrin. *EMBO J.* **2007**, *26*, 1129–1139.

(82) Yan, S. D.; Chen, X.; Fu, J.; Chen, M.; Zhu, H.; Roher, A.; Slattey, T.; Zhao, L.; Nagashima, M.; Morser, J.; Migheli, A.; Nawroth, P.; Stern, D.; Schmidt, A. M. RAGE and amyloid-beta peptide neurotoxicity in Alzheimer's disease. *Nature* **1996**, *382*, 685–691.

(83) Chaney, M. O.; Stine, W. B.; Kokjohn, T. A.; Kuo, Y. M.; Esh, C.; Rahman, A.; Luehrs, D. C.; Schmidt, A. M.; Stern, D.; Yan, S. D.; Roher, A. E. RAGE and amyloid beta interactions: atomic force microscopy and molecular modeling. *Biochim. Biophys. Acta, Mol. Basis Dis.* **2005**, *1741*, 199–205.

(84) Deane, R.; Du Yan, S.; Subramanian, R. K.; LaRue, B.; Jovanovic, S.; Hogg, E.; Welch, D.; Manness, L.; Lin, C.; Yu, J.; Zhu, H.; Ghiso, J.; Frangione, B.; Stern, A.; Schmidt, A. M.; Armstrong, D. L.; Arnold, B.; Liliensiek, B.; Nawroth, P.; Hofman, F.; Kindy, M.; Stern, D.; Zlokovic, B. RAGE mediates amyloid-beta peptide transport across the blood-brain barrier and accumulation in brain. *Nat. Med.* **2003**, *9*, 907–913.

(85) Yan, S. D.; Stern, D.; Kane, M. D.; Kuo, Y. M.; Lampert, H. C.; Roher, A. E. RAGE-Abeta interactions in the pathophysiology of Alzheimer's disease. *Restor. Neurol. Neurosci.* **1998**, *12*, 167–173.

(86) Lugo-Huitron, R.; Ugalde Muniz, P.; Pineda, B.; Pedraza-Chaverri, J.; Rios, C.; Perez-de la Cruz, V. Quinolinic acid: an endogenous neurotoxin with multiple targets. *Oxid. Med. Cell. Longevity* **2013**, *2013*, 104024.

(87) Serratos, I. N.; Castellanos, P.; Pastor, N.; Millán-Pacheco, C.; Rembao, D.; Pérez-Montfort, R.; Cabrera, N.; Reyes-Espinosa, F.; Díaz-Garrido, P.; López-Macay, A.; Martínez-Flores, K.; López-Reyes, A.; Sánchez-García, A.; Cuevas, E.; Santamaria, A. Modeling the Interaction between Quinolate and the Receptor for Advanced Glycation End Products (RAGE): Relevance for Early Neuro-pathological Processes. *PLoS One* **2015**, *10*, e0120221.

(88) Cuevas, E.; Lantz, S.; Newport, G.; Divine, B.; Wu, Q.; Paule, M. G.; Tobon-Velasco, J. C.; Ali, S. F.; Santamaria, A. On the early toxic effect of quinolinic acid: involvement of RAGE. *Neurosci. Lett.* **2010**, *474*, 74–78.

(89) Yamamoto, K.; Murata, H.; Putranto, E. W.; Kataoka, K.; Motoyama, A.; Hibino, T.; Inoue, Y.; Sakaguchi, M.; Huh, N. H. DOCK7 is a critical regulator of the RAGE-Cdc42 signaling axis that induces formation of dendritic pseudopodia in human cancer cells. *Oncol. Rep.* **2013**, *29*, 1073–1079.

(90) Lin, Y. N.; Bhuwania, R.; Gromova, K.; Failla, A. V.; Lange, T.; Riecken, K.; Linder, S.; Kneussel, M.; Izbicki, J. R.; Windhorst, S. Drosophila homologue of Diaphanous 1 (DIAPH1) controls the metastatic potential of colon cancer cells by regulating microtubule-dependent adhesion. *Oncotarget* **2015**, *6*, 18577–18589.

(91) Chen, S. C.; Guh, J. Y.; Hwang, C. C.; Chiou, S. J.; Lin, T. D.; Ko, Y. M.; Huang, J. S.; Yang, Y. L.; Chuang, L. Y. Advanced glycation end-products activate extracellular signal-regulated kinase via the oxidative stress-EGF receptor pathway in renal fibroblasts. *J. Cell. Biochem.* **2010**, *109*, 38–48.

(92) Zhou, Y.; Johnson, J. L.; Cerione, R. A.; Erickson, J. W. Prenylation and membrane localization of Cdc42 are essential for activation by DOCK7. *Biochemistry* **2013**, *52*, 4354–4363.

(93) Brett, J.; Schmidt, A. M.; Yan, S. D.; Zou, Y. S.; Weidman, E.; Pinsky, D.; Nowygrod, R.; Neeper, M.; Przysiecki, C.; Shaw, A.; et al. Survey of the distribution of a newly characterized receptor for advanced glycation end products in tissues. *Am. J. Pathol.* **1993**, *143*, 1699–1712.

(94) Wendt, T.; Harja, E.; Bucciarelli, L.; Qu, W.; Lu, Y.; Rong, L. L.; Jenkins, D. G.; Stein, G.; Schmidt, A. M.; Yan, S. F. RAGE modulates vascular inflammation and atherosclerosis in a murine model of type 2 diabetes. *Atherosclerosis* **2006**, *185*, 70–77.

(95) Ahmed, N. Advanced glycation endproducts—role in pathology of diabetic complications. *Diabetes Res. Clin. Pract.* **2005**, *67*, 3–21.

(96) Uchida, T.; Shirasawa, M.; Ware, L. B.; Kojima, K.; Hata, Y.; Makita, K.; Mednick, G.; Matthay, Z. A.; Matthay, M. A. Receptor for

advanced glycation end-products is a marker of type I cell injury in acute lung injury. *Am. J. Respir. Crit. Care Med.* **2006**, *173*, 1008–1015.

(97) Buckley, S. T.; Ehrhardt, C. The receptor for advanced glycation end products (RAGE) and the lung. *J. Biomed. Biotechnol.* **2010**, *2010*, 917108.

(98) Zeng, S.; Cataldegirmen, G.; Feirt, N.; Ippagunta, N.; Dun, H.; Wu, Q.; Yan, L.; Rong, L. L.; Yan, S. F.; Schmidt, A. M.; Emond, J. C. RAGE limits regeneration after massive liver injury by coordinated suppression of TNF-alpha and NF-KB. *Hepatology* **2004**, *40*, 284a–285a.

(99) Liu, Y.; Liang, C.; Liu, X.; Liao, B.; Pan, X.; Ren, Y.; Fan, M.; Li, M.; He, Z.; Wu, J.; Wu, Z. AGEs increased migration and inflammatory responses of adventitial fibroblasts via RAGE, MAPK and NF-kappaB pathways. *Atherosclerosis* **2010**, *208*, 34–42.

(100) Yeh, C. H.; Sturgis, L.; Haidacher, J.; Zhang, X. N.; Sherwood, S. J.; Bjerkke, R. J.; Juhasz, O.; Crow, M. T.; Tilton, R. G.; Denner, L. Requirement for p38 and p44/p42 mitogen-activated protein kinases in RAGE-mediated nuclear factor-kappaB transcriptional activation and cytokine secretion. *Diabetes* **2001**, *50*, 1495–1504.

(101) Perkins, N. D. Integrating cell-signalling pathways with NF-kappaB and IKK function. *Nat. Rev. Mol. Cell Biol.* **2007**, *8*, 49–62.

(102) Chen, C. H.; Zhou, W.; Liu, S.; Deng, Y.; Cai, F.; Tone, M.; Tone, Y.; Tong, Y.; Song, W. Increased NF-kappaB signalling up-regulates BACE1 expression and its therapeutic potential in Alzheimer's disease. *Int. J. Neuropsychopharmacol.* **2012**, *15*, 77–90.

(103) Bianchi, R.; Giambanco, I.; Donato, R. S100B/RAGE-dependent activation of microglia via NF-kappaB and AP-1 Co-regulation of COX-2 expression by S100B, IL-1beta and TNF-alpha. *Neurobiol. Aging* **2010**, *31*, 665–677.

(104) Chen, X.; Zhang, L.; Zhang, I. Y.; Liang, J.; Wang, H.; Ouyang, M.; Wu, S.; da Fonseca, A. C.; Weng, L.; Yamamoto, Y.; Yamamoto, H.; Natarajan, R.; Badie, B. RAGE expression in tumor-associated macrophages promotes angiogenesis in glioma. *Cancer Res.* **2014**, *74*, 7285–7297.

(105) Fuentes, M. K.; Nigavekar, S. S.; Arumugam, T.; Logsdon, C. D.; Schmidt, A. M.; Park, J. C.; Huang, E. H. RAGE activation by S100P in colon cancer stimulates growth, migration, and cell signaling pathways. *Dis. Colon Rectum* **2007**, *50*, 1230–1240.

(106) Kislinger, T.; Tanji, N.; Wendt, T.; Qu, W.; Lu, Y.; Ferran, L. J., Jr.; Taguchi, A.; Olson, K.; Bucciarelli, L.; Goova, M.; Hofmann, M. A.; Cataldegirmen, G.; D'Agati, V.; Pischetsrieder, M.; Stern, D. M.; Schmidt, A. M. Receptor for advanced glycation end products mediates inflammation and enhanced expression of tissue factor in vasculature of diabetic apolipoprotein E-null mice. *Arterioscler., Thromb., Vasc. Biol.* **2001**, *21*, 905–910.

(107) Ramasamy, R.; Yan, S. F.; Schmidt, A. M. Receptor for AGE (RAGE): signaling mechanisms in the pathogenesis of diabetes and its complications. *Ann. N. Y. Acad. Sci.* **2011**, *1243*, 88–102.

(108) Coughlan, M. T.; Thorburn, D. R.; Penfold, S. A.; Laskowski, A.; Harcourt, B. E.; Sourris, K. C.; Tan, A. L.; Fukami, K.; Thallas-Bonke, V.; Nawroth, P. P.; Brownlee, M.; Bierhaus, A.; Cooper, M. E.; Forbes, J. M. RAGE-induced cytosolic ROS promote mitochondrial superoxide generation in diabetes. *J. Am. Soc. Nephrol.* **2009**, *20*, 742–752.

(109) Aleshin, A.; Ananthakrishnan, R.; Li, Q.; Rosario, R.; Lu, Y.; Qu, W.; Song, F.; Bakr, S.; Szabolcs, M.; D'Agati, V.; Liu, R.; Homma, S.; Schmidt, A. M.; Yan, S. F.; Ramasamy, R. RAGE modulates myocardial injury consequent to LAD infarction via impact on JNK and STAT signaling in a murine model. *Am. J. Physiol.: Heart Circ. Physiol.* **2008**, *294*, H1823–1832.

(110) Chung, J.; An, S. H.; Kang, S. W.; Kwon, K. Ursodeoxycholic Acid (UDCA) Exerts Anti-Atherogenic Effects by Inhibiting RAGE Signaling in Diabetic Atherosclerosis. *PLoS One* **2016**, *11*, e0147839.

(111) Hudson, B. I.; Bucciarelli, L. G.; Wendt, T.; Sakaguchi, T.; Lalla, E.; Qu, W.; Lu, Y.; Lee, L.; Stern, D. M.; Naka, Y.; Ramasamy, R.; Yan, S. D.; Yan, S. F.; D'Agati, V.; Schmidt, A. M. Blockade of receptor for advanced glycation endproducts: a new target for therapeutic intervention in diabetic complications and inflammatory disorders. *Arch. Biochem. Biophys.* **2003**, *419*, 80–88.

(112) Deane, R. J. Is RAGE still a therapeutic target for Alzheimer's disease? *Future Med. Chem.* **2012**, *4*, 915–925.

(113) Miller, M. C.; Tavares, R.; Johanson, C. E.; Hovanesian, V.; Donahue, J. E.; Gonzalez, L.; Silverberg, G. D.; Stopa, E. G. Hippocampal RAGE immunoreactivity in early and advanced Alzheimer's disease. *Brain Res.* **2008**, *1230*, 273–280.

(114) Sasaki, N.; Toki, S.; Chowei, H.; Saito, T.; Nakano, N.; Hayashi, Y.; Takeuchi, M.; Makita, Z. Immunohistochemical distribution of the receptor for advanced glycation end products in neurons and astrocytes in Alzheimer's disease. *Brain Res.* **2001**, *888*, 256–262.

(115) Jeynes, B.; Provias, J. Evidence for altered LRP/RAGE expression in Alzheimer lesion pathogenesis. *Curr. Alzheimer Res.* **2008**, *5*, 432–437.

(116) Donahue, J. E.; Flaherty, S. L.; Johanson, C. E.; Duncan, J. A., 3rd; Silverberg, G. D.; Miller, M. C.; Tavares, R.; Yang, W.; Wu, Q.; Sabo, E.; Hovanesian, V.; Stopa, E. G. RAGE, LRP-1, and amyloid-beta protein in Alzheimer's disease. *Acta Neuropathol.* **2006**, *112*, 405–415.

(117) Li, X. H.; Lv, B. L.; Xie, J. Z.; Liu, J.; Zhou, X. W.; Wang, J. Z. AGEs induce Alzheimer-like tau pathology and memory deficit via RAGE-mediated GSK-3 activation. *Neurobiol. Aging* **2012**, *33*, 1400–1410.

(118) Guglielmotto, M.; Aragno, M.; Tamagno, E.; Vercellinato, I.; Visentin, S.; Medana, C.; Catalano, M. G.; Smith, M. A.; Perry, G.; Danni, O.; Boccuzzi, G.; Tabaton, M. AGEs/RAGE complex upregulates BACE1 via NF-kappaB pathway activation. *Neurobiol. Aging* **2012**, *33*, 196.e13–196.327.

(119) Kumar, A.; Singh, A.; Ekavali. A review on Alzheimer's disease pathophysiology and its management: an update. *Pharmacol. Rep.* **2015**, *67*, 195–203.

(120) Takuma, K.; Fang, F.; Zhang, W.; Yan, S.; Fukuzaki, E.; Du, H.; Sosunov, A.; McKhann, G.; Funatsu, Y.; Nakamichi, N.; Nagai, T.; Mizoguchi, H.; Ibi, D.; Hori, O.; Ogawa, S.; Stern, D. M.; Yamada, K.; Yan, S. S. RAGE-mediated signaling contributes to intraneuronal transport of amyloid-beta and neuronal dysfunction. *Proc. Natl. Acad. Sci. U. S. A.* **2009**, *106*, 20021–20026.

(121) Burstein, A. H.; Grimes, I.; Galasko, D. R.; Aisen, P. S.; Sabbagh, M.; Mjalli, A. M. Effect of TTP488 in patients with mild to moderate Alzheimer's disease. *BMC Neurol.* **2014**, *14*, 12.

(122) Sabbagh, M. N.; Agro, A.; Bell, J.; Aisen, P. S.; Schweizer, E.; Galasko, D. PF-04494700, an oral inhibitor of receptor for advanced glycation end products (RAGE), in Alzheimer disease. *Alzheimer Dis. Assoc. Disord.* **2011**, *25*, 206–212.

(123) Lee, Y. S.; Kim, H.; Kim, Y. H.; Roh, E. J.; Han, H.; Shin, K. J. Synthesis and structure-activity relationships of tri-substituted thiazoles as RAGE antagonists for the treatment of Alzheimer's disease. *Bioorg. Med. Chem. Lett.* **2012**, *22*, 7555–7561.

(124) Han, Y. T.; Choi, G. I.; Son, D.; Kim, N. J.; Yun, H.; Lee, S.; Chang, D. J.; Hong, H. S.; Kim, H.; Ha, H. J.; Kim, Y. H.; Park, H. J.; Lee, J.; Suh, Y. G. Ligand-based design, synthesis, and biological evaluation of 2-aminopyrimidines, a novel series of receptor for advanced glycation end products (RAGE) inhibitors. *J. Med. Chem.* **2012**, *55*, 9120–9135.

(125) Kim, S. H.; Han, Y. T. Design, synthesis, and biological evaluation of pyrimidine-2-carboxamide analogs: investigation for novel RAGE inhibitors with reduced hydrophobicity and toxicity. *Arch. Pharmacol. Res.* **2015**, *38*, 1952–1962.

(126) Han, Y. T.; Kim, K.; Son, D.; An, H.; Kim, H.; Lee, J.; Park, H. J.; Lee, J.; Suh, Y. G. Fine tuning of 4,6-bisphenyl-2-(3-alkoxyanilino)-pyrimidine focusing on the activity-sensitive aminoalkoxy moiety for a therapeutically useful inhibitor of receptor for advanced glycation end products (RAGE). *Bioorg. Med. Chem.* **2015**, *23*, 579–587.

(127) Han, Y. T.; Kim, K.; Choi, G. I.; An, H.; Son, D.; Kim, H.; Ha, H. J.; Son, J. H.; Chung, S. J.; Park, H. J.; Lee, J.; Suh, Y. G. Pyrazole-5-carboxamides, novel inhibitors of receptor for advanced glycation end products (RAGE). *Eur. J. Med. Chem.* **2014**, *79*, 128–142.

(128) Choi, K.; Lim, K. S.; Shin, J.; Kim, S. H.; Suh, Y. G.; Hong, H. S.; Kim, H.; Ha, H. J.; Kim, Y. H.; Lee, J.; Lee, J. 6-Phenoxy-2-phenylbenzoxazoles, novel inhibitors of receptor for advanced

glycation end products (RAGE). *Bioorg. Med. Chem.* **2015**, *23*, 4919–4935.

(129) Mjalli, A. M. M.; Andrews, R. C.; Gopalaswamy, R.; Wysong, C. Carboxamide Derivatives as Therapeutic Agents. WO2002070473, 2002.

(130) Mjalli, A. M. M.; Gopalaswamy, R.; Avor, K.; Wysong, C.; Patron, A. Method for the Synthesis of Compounds of Formula I and Their Uses Thereof. WO2001092210, 2002.

(131) Mjalli, A. M. M.; Andrews, R. C.; Gopalaswamy, R.; Hari, A.; Avor, K.; Qabaja, G.; Guo, X. C.; Gupta, S.; Jones, D. R.; Chen, X. Mono- and Bicyclic Azole Derivatives that Inhibit the Interaction of Ligands with RAGE. WO2003075921, 2003.

(132) Mjalli, A. M. M.; Gopalaswamy, R. Benzimidazole Derivatives as Therapeutic Agents. WO2002069965, 2003.

(133) Ross, N. T.; Deane, R.; Perry, S.; Miller, B. L. Structure–activity relationships of small molecule inhibitors of RAGE- β binding. *Tetrahedron* **2013**, *69*, 7653–7658.

(134) Gu, Q.; Wang, B.; Zhang, X. F.; Ma, Y. P.; Liu, J. D.; Wang, X. Z. Contribution of receptor for advanced glycation end products to vasculature-protecting effects of exercise training in aged rats. *Eur. J. Pharmacol.* **2014**, *741*, 186–194.

(135) Cui, L.; Cai, Y.; Cheng, W.; Liu, G.; Zhao, J.; Cao, H.; Tao, H.; Wang, Y.; Yin, M.; Liu, T.; Liu, Y.; Huang, P.; Liu, Z.; Li, K.; Zhao, B. A Novel, Multi-Target Natural Drug Candidate, Matrine, Improves Cognitive Deficits in Alzheimer's Disease Transgenic Mice by Inhibiting A β Aggregation and Blocking the RAGE/A β Axis. *Mol. Neurobiol.* **2017**, *54*, 1939–1952.

(136) Mizumoto, S.; Takahashi, J.; Sugahara, K. Receptor for advanced glycation end products (RAGE) functions as receptor for specific sulfated glycosaminoglycans, and anti-RAGE antibody or sulfated glycosaminoglycans delivered in vivo inhibit pulmonary metastasis of tumor cells. *J. Biol. Chem.* **2012**, *287*, 18985–18994.

(137) Zhang, J.; Xu, X.; Rao, N. V.; Argyle, B.; McCoard, L.; Rusho, W. J.; Kennedy, T. P.; Prestwich, G. D.; Krueger, G. Novel sulfated polysaccharides disrupt cathelicidins, inhibit RAGE and reduce cutaneous inflammation in a mouse model of rosacea. *PLoS One* **2011**, *6*, e16658.

(138) Arumugam, T.; Ramachandran, V.; Gomez, S. B.; Schmidt, A. M.; Logsdon, C. D. S100P-derived RAGE antagonistic peptide reduces tumor growth and metastasis. *Clin. Cancer Res.* **2012**, *18*, 4356–4364.

(139) Schmidt, A. M.; Ramasamy, R.; Shekhtman, A.; Rai, V.; Manigrasso, M. B. Amido and Heterocyclic Compounds as Modulators of RAGE Activity and Uses Thereof. WO2015050984, 2014.

(140) Kim, S. J.; Ahn, J. W.; Kim, H.; Ha, H. J.; Lee, S. W.; Kim, H. K.; Lee, S.; Hong, H. S.; Kim, Y. H.; Choi, C. Y. Two beta-strands of RAGE participate in the recognition and transport of amyloid-beta peptide across the blood brain barrier. *Biochem. Biophys. Res. Commun.* **2013**, *439*, 252–257.

(141) Mohan, S. K.; Gupta, A. A.; Yu, C. Interaction of the S100A6 mutant (C3S) with the V domain of the receptor for advanced glycation end products (RAGE). *Biochem. Biophys. Res. Commun.* **2013**, *434*, 328–333.

(142) Yatime, L.; Betzer, C.; Jensen, R. K.; Mortensen, S.; Jensen, P. H.; Andersen, G. R. The Structure of the RAGE:S100A6 Complex Reveals a Unique Mode of Homodimerization for S100 Proteins. *Structure* **2016**, *24*, 2043–2052.

(143) Jones, D.; Gowda, R. B.; Xie, R. Substituted Imidazole Derivatives for Treatment of Alzheimers Disease. WO2011041198, 2012.

(144) Mjalli, A. M. M.; Andrews, R. C.; Shen, J. M.; Rothlein, R. RAGE Antagonists as Agents to Reverse Amyloidosis and Diseases Associated Therewith. WO2005000295, 2009.